



Combining Super-Resolution and Level Sets for Brain Image Segmentation

Farzaneh Elahifasae

Department of Signals and systems, Signal Processing Group
Chalmers University of Technology
Gothenburg, Sweden 2012
Report No.EX013/2012

Abstract

The term Super resolution, resolution enhancement, is a process to increase the resolution of an image. This improvement quality is due to sub-pixel shift of low resolution images from each other between images.

In fact, each low resolution image has new information of the image and the main aim of super resolution is to combining these low resolution images to enhance the image resolution.

Following this method, allows users that without any demand for additional hardware, overcoming the limitations of the imaging system.

Moreover, the main goal of segmentation is to distinguish an object from background. Segmentation can do that by dividing pixels of an image into prominent image regions. By this way, a specific region is corresponding to individual objects or natural parts of objects. Segmentation can be used in different fields such as image compression and image editing.

Various methods have been proposed to enhance the segmentation results. In this thesis combining super resolution and level set segmentation were compared to low resolution images segmentation.

The results show that segmentation of super resolution image has better result compared to segmentation of low resolution images.

Acknowledgements

I would like to thank my advisor Prof. Irene Gu for her patience, guidance, and mentorship throughout my thesis. It means a lot to me to have someone looking out for me and providing this opportunity to work under her supervision. I give special thanks to her for introducing this field of research to me and for her beneficial comments and insight throughout the thesis that makes me deeper, more efficient and more productive.

Last but not least, I am grateful to my family and friends for their emotional support in these sometimes difficult years.

Farzaneh Elahifasae, Goteborg 12/02/1

Contents

1	Introduction	1
2	Theory and background	4
2.1	SR image reconstruction	4
2.2	Previous works	6
2.2.1	super resolution in frequency domain	6
2.2.2	Spatial domain methods	7
2.2.3	Projection and interpolation	7
2.2.4	Probabilistic methods	7
2.2.5	Iterative method	7
2.2.6	Projection on to convex sets	8
2.2.7	Edge-preservation method	8
2.3	Model	9
2.3.1	Registration	11
2.3.2	Interpolation	12
2.3.3	De-blurring and De-noising	15
2.4	Segmentation	16
2.4.1	Active contour model (Snakes)	16
2.4.2	Model-based active contour	17
2.4.3	Region based level set for segmentation	17
2.4.4	Multiphase level set formulation	19
2.4.5	Image segmentation as Bayesian inference	20
2.4.6	Level set method and image segmentation	23
3	Softwares	25
3.1	SR image reconstruction Software	25
3.1.1	Motion Estimation Algorithms	26
3.1.2	Reconstruction Algorithm	27
3.2	Level set segmentation software	30

4	Testing a super-resolution image segmentation method	33
5	Experiment results	34
5.1	Segmentation evaluation	34
5.2	Experimental set-up	35
5.3	Experiment results	36
5.3.1	Example 1	36
5.3.2	Example 2	38
5.3.3	Example 3	40
5.3.4	Example 4	42
5.3.5	Example 5	44
5.3.6	Example 6	46
5.3.7	Example 7	48
5.3.8	Example 8	50
5.3.9	Example 9	52
5.3.10	Example 10	54
5.3.11	Example 11	56
5.3.12	Example 12	58
6	Conclusion	61

1

Introduction

Super resolution(SR) is the term used to refer to the image processing done to obtain a high resolution(HR) image from multiple low resolution(LR) images. Super resolution techniques are applied on multiple LR images captured from the same scene in order to increase spatial resolution for a new image of that same scene.

That is, LR images are sub sampled(aliasd) as well as shifted with sub pixel precision. If LR images are shifted by integer units, then each image contains the same information, and then there is no new information that can be used to reconstruct a HR image.

If the LR images have different sub pixel shifts from each other and if aliasing is present then each image can not be obtained from the others. In this case, the new information contained in each LR image can be exploited to obtain a HR image.

To obtain different looks at the same scene, some relative scene motions most exists from frame to frame from multiple scenes or video sequences. Multiple scenes can be obtained from one camera with several captures or from multiple cameras located indifferent positions.

Frame also can be obtained of one scene but from video sequence. If these scene motion are known or can be estimated with sub pixel accuracy and then by combining these LR images, SR image reconstruction is possible as illustrated in figure 1.1.

Main aim of image segmentation is to partition an image into meaningful regions. As a matter of fact, segmentation is based on measurements taken from the image and might be gray level, color and motion.

Usually image segmentation is an initial and vital step in a series of processes aimed at overall image understanding. All in all, blurring factors and discretizing process also hamper reliable segmentation and subsequent analysis. The result of image segmentation is a set of segments that collectively cover the entire image, or a set of contours extracted from the image. Each of pixels in a regions are similar with respect to the same characteristics.

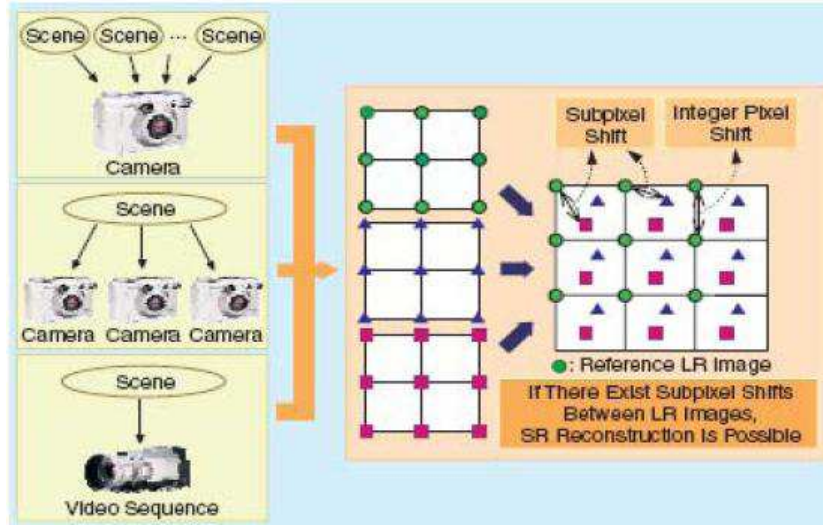


Figure 1.1: Basic concept for super resolution. This figure is from[1]

The process of segmentation is directly tried to recognition and it is likely that to achieve a complete separation of objects from background, information that can only be obtained from higher level recognition, interference and perceptual completion procedure will be required.

Two major segmentation methods that were used in recent years for image segmentation are "Mean shift" and "Normalized cut" segmentation, each of them has its own pros and cons as below:

- Just simple parameter(window size)is used in this method.
- Robust to outliers and finds variable number of modes.

Moreover following disadvantages considered for this scheme:

- Output depends on window size.
- Does not scale well with dimension of feature space.

Meanwhile, normalized cut method benefits can be considered as:
Can be used with many different features and affinity formulation.
Furthermore, normalized cuts drawback can be considered as:

- High storage requirement.
- time complexity.
- Bias towards partitioning into equal segments.

The proposed segmentation technique use level set scheme. Actually, the main motivation for investigation level set is to achieve better result from segmentation compared to traditional approach.

The idea behind level set is to specification an initial contour which is moved by internal and external forces to boundaries of the desired object. During the deformation process, the internal force tries to keep the model smooth, while external force move the model forward an object boundary.

Using level set encodes numerous advantages as below:

- Bias towards partitioning into equal segments.
- This method provides a direct way to estimate the geometric properties of the evolving structure.
- It can be used as a optimization framework.
- Topology can be change using this scheme.
- This method is free parameter and intrinsic.

In this thesis the results of applying one specific segmentation method, region scalable fitting energy, on low resolution and high resolution images has been compared. The results indicating that segmentation has far better outcome on super resolution images. Remaining chapters are arranged as follows:

Chapter 2 Reviews background theories in super resolution image reconstruction and segmentation.

Chapter 3 Softwares.

Chapter 4 Testing a super-resolution image segmentation method.

Chapter 5 Experimental results.

Chapter 6 Conclusion.

2

Theory and background

Generally speaking, the main goal of this thesis is to find an optimum way for image segmentation. Our suggestion is a way to apply segmentation on super resolution images. At this chapter, we have some brief review of basics of super resolution and segmentation.

2.1 SR image reconstruction

It has been well around three decades from since the first attempts on image processing by computer. The most crucial reason to this effort is that the majority of data that human being receive is by his observation and image processing techniques are applied in a wide variety of fields, like medical imaging, surveillance, robotics, industrial inception and remote sensing.[2]

So, in many applications the demand for highly detailed images, is gradually increasing. High resolution means that the number of pixels within a given size of image is large. Therefore a high resolution image usually offers important or even critical information for various practical applications.[3]

Although charge coupled device (CCD) and CMOS image sensors have been widely used in recent decades, but the current resolution level in these sensors does not meet the increasing demands in the near future because as the resolution of a camera sensor increase, it would be more expensive. In this way, finding an effective way to increase image resolution is a matter of importance. One simple solution to increase spatial resolution of low resolution images is to reduce the pixel size by sensor manufacturing techniques. However, as the pixel size decreases, the power of the light incident to each single photo detector also decreases that causes degrading of image quality by insufficient signal to noise ratio so it is impossible to have high resolution image by reducing the size of pixels[4].

Another technique is to improve the spatial resolution of low resolution images. Main

aim of this approach is to increase the size of sensor chip that leads to lower charge transfer rate and a longer period of time to capture an image. So, this method is not acceptable for cost effective commercial applications.

All in all, it is often not feasible or sometimes possible to acquire images of such high resolution by just using hardware[5].

In many imaging systems, however, the quality of image resolution is limited by physical constraints. The imaging systems yield aliased and under sampled images if their detector array is not sufficiently dense. So, digital image processing approaches have been investigated to reconstruct a high-resolution image from multiple degraded low-resolution images.

Actually, by using super resolution algorithms, high resolution images can be reconstructed from a series of low resolution images and the idea behind this concept is to combine the information from a set of undersampled(aliased) low resolution images of the same scene and use it to construct a high resolution image or image sequence.[6].

Many reconstruction methods have been proposed over the years but, must super resolution reconstruction methods employ following steps: image registration, interpolation and optional restoration (deblurring, denoising). Some methods perform these tasks separately, while others combine two or more of them.

In following we would have a take a look at historical improvement of super resolution technique.

2.2 Previous works

In following we would have a take a look at historical improvement of super resolution technique.

2.2.1 super resolution in frequency domain

Tsai and Hung were the first to consider the problem attaining a high resolution image from mixing a set of low resolution images. Their data set had been achieved by Landset Satellite photographs. They modelled the images as aliased translationally displaced versions of a constant scene. They had been used from discrete time Fourier transform in their method. It can be said that their approach was based on the 3 following items:

1. Shifting property of the Fourier Transformation.
2. Aliasing relationship between continuous Fourier transform and high resolution image.
3. Band limited high resolution image.

Figure (2.1) represent aliasing relationship between low resolution image and high resolution image.

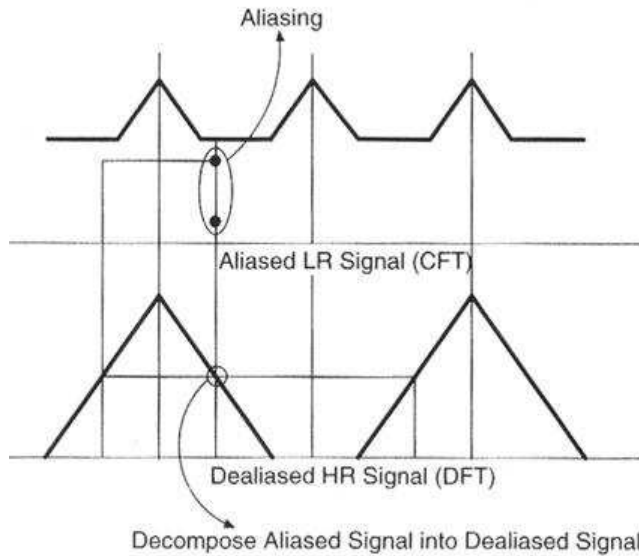


Figure 2.1: Aliasing relationship between LR and HR image. This figure is from [1]

But, they did not consider noise and optical blur in their method. Ozkan, Tekalp and Sezan by using noise and point spread function, extended Tsai and Haung formulation. Kim, Bose and Valenzuelan also used the model of Tsai and Haung but with

consideration of noise and blur. The drawback with their technique was that because of presence of zeroes in the PSF, this method was ill-posedness. Moreover, the mention estimation was not considered in their method.

2.2.2 Spatial domain methods

Actually, most of research that has been done in super resolution field is in this class of reconstruction methods and the reason for that is firstly, the constraints are much easier to formulate and secondly, this technique include a great flexibility in in the motion model, motion blur, optical blur and the sampling process.

2.2.3 Projection and interpolation

If ideal sampling is considered, then our issue reduces essentially to projection a high resolution grid and interpolating of non uniformly spaced samples. Comparison between different interpolation methods with high resolution reconstruction results can be found in [2] and [7].

2.2.4 Probabilistic methods

Modelling of images as probability distribution seems to be acceptable because super resolution has been relaying on the approximation of parameters and data that are unknown. Schultz and Svensson [8] used Huber Markov random fields in Bayesian framework to clarify discontinuity preserving prior image density function.

MAP estimation that relate on to independent motion is done by gradient projection algorithm is considered. Motion estimation error is also considered as probability density function.

Hardie, Barnard and Armstrong also followed the Schultz and Svensson but, they made a difference by estimating the high resolution image and motion parameters at the same time. In fact, their work had the advantage of of not estimating motion directly from low resolution images.

Moreover, Tom and Katasgelesb [5] instead of MAP approach used ML method to reduce blur and noise. By utilizing exception maximization technique they can obtain registration and restoration concurrently.

2.2.5 Iterative method

The iterative methods are the most important technique in spatial domain methods. the benefits of this technique is the possibility of dealing with vast range of data(images)sequence, easy inclusion of spatial domain and the capability of this technique to utilizing varying degradation.

Actually, by the iteration technique first of all we make a rough guess and then try to achieve successfully more developed estimation.

As a matter of fact, there are so many iterative techniques to solve super resolution reconstruction methods.

Feuer and Elad use different approximation to the Kalman filter and estimate its performance by Recursive Least Square(RLS), Least Mean Square(LMS) and Steepest Descent(SD). Irani and Peleg introduced the Iterative Back Projection(IBM) algorithm oriented from computer aided tomography(CAT).

To decrease the ill posedness and noise Stack et.al. applied a set of theoretic algorithm projection on to convex sets(POCS). Peleg and Irani modify their method to deal with more complex motion types like local motion partial occlusion and transparency. Shah and Zakhor also followed the Peleg and Irani and proposed a novel approach for motion estimation.

2.2.6 Projection on to convex sets

This technique is an alternative iterative method to have a feature based on prior knowledge about possible solution into the reconstruction process. Actually this approach approximates the super resolution image based on finding solution for the problem of interpolation and restoration.

This method was first introduced by Oskoui and Stark[9]. They used from convexity and closeness of the constraint sets to ensure convergence of iterativity projecting the images on to the sets; but their solution has some drawbacks. For example, it was dependence of initial guess and it was non-unique.

Takalp et.al. then used from Oskoui and Stark formulation and make that more robust by considering the observation noise and the motion blur[10].

Based on the POCS method incorporating a priori knowledge into the solution can be represented as a limit to solution to be a member of a closed convex set C_i which can be expressed as a set of vectors that satisfy a specific property. If the limiting sets have a non-empty intersection, then a solution that belongs to the intersection set C_s can be found by projections onto those convex sets.

The advantage of POCS method is that it uses from strong spatial domain observation model. Moreover, its simplicity and flexibility should not be ignored. Furthermore, some problems with this technique is having a high computational cost, slow convergence and non-uniqueness[1].

Peleg and Irani modify their method to deal with more complex motion types like local motion partial occlusion and transparency. Shah and Zakhor also followed the Peleg and Irani and proposed a novel approach for motion estimation.

2.2.7 Edge-preservation method

Milanfar et.al. proposed using the L_1 norm in the super resolution both for data fusion and for the image registration.

L_1 norm has the capability of removing outlier efficiently. Moreover, it performs spatially well in facing with non-Gaussian noise. Furthermore, the results that achieved by L_1 norm approach are less sensitive to the outlier in the super resolution images.

2.3 Model

The concept of super resolution is based on achieving high resolution image the noisy, blurred and aliased image. The cause of degradation are: Optical blur, Noise and Aliasing effects.

Below figure shows the degradation of the low resolution image that used by the recording process.

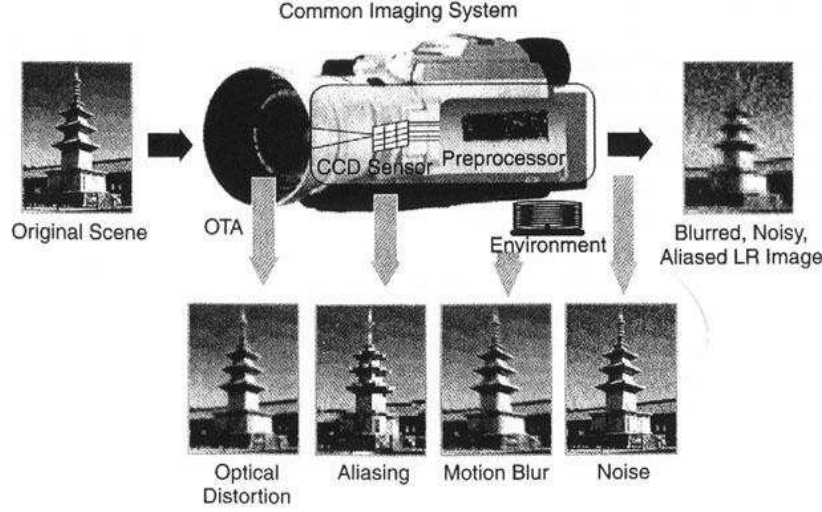


Figure 2.2: Degradations of low resolution image caused by the recording process. This figure is from [1]

For analysing the super resolution image comprehensively, having formulation that relates high resolution model to the observed low resolution image is a must. Observation model can be represented as below:

$$\mathbf{Y}_k = DB_k M_k X + n_k \quad (2.1)$$

A block diagram for the observation model was illustrated in figure(2.2)

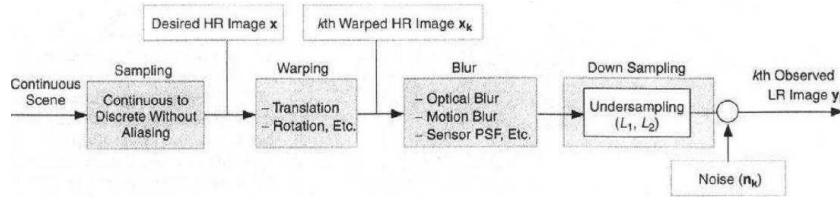


Figure 2.3: Model for observed low resolution image. This figure is from [1]

D_k is considered as a sub-sampling matrix that can generates images from the warped and blurred high resolution images. Actually by using sub-sampling different size of low

resolution images can be achieved.

M_k is the warp matrix is due to the motion that occurs during image possessions. This factor consists of a rotation and transformation and so on. Figure(2.3)shows why interpolation is necessary in our high resolution image.

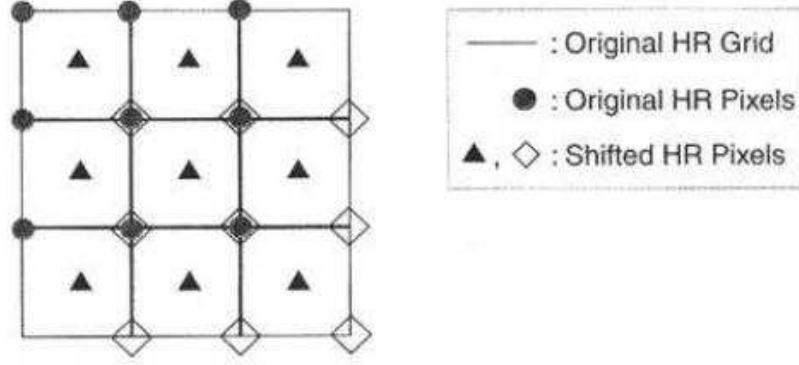


Figure 2.4: Interpolation from frame to frame. This figure is from [1]

B_k is the blur matrix because of relative motion between the imaging system and original scene or optical system such as aberration and out of focus. Blur can also caused by point spread function (PSF) of the low resolution sensor which can be modelled as a special averaging operator.

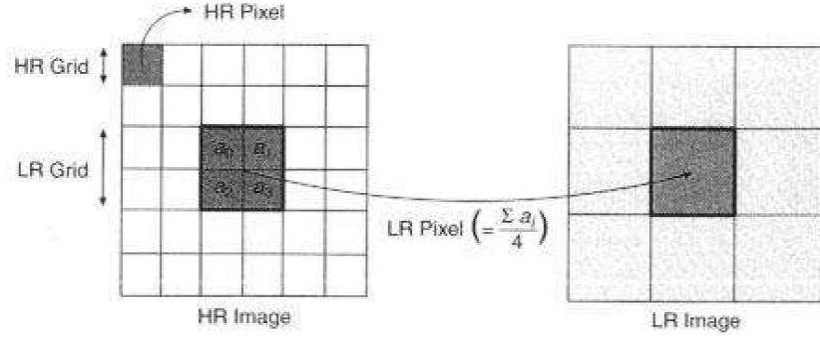


Figure 2.5: Low resolution sensor's PSF. This figure is from [1]

In summary, super resolution reconstruction of images can be sub-divided into three parts: Registration, interpolation and De-blurring and De-noising.

Figure(2.6)shows those three steps for super resolution. It is worth mentioning that these major parts dependent on the deconstruction method, can be implemented individually or simultaneously.

In the the following a brief description of these three items are presented.

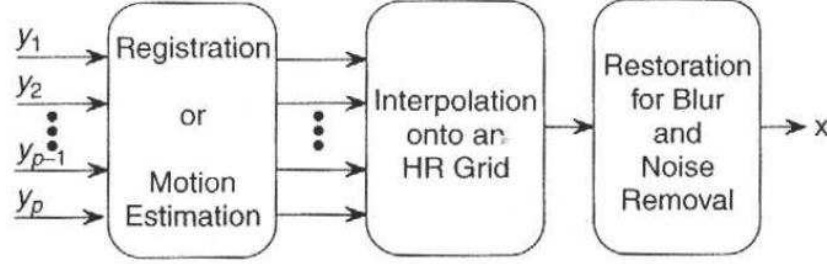


Figure 2.6: Major steps during super resolution reconstruction. This figure is from [1]

2.3.1 Registration

Image registration is the process of covering two or more images that taken from the same scene but at different time, from different viewpoint or with different sensors.

Image registration in different time or multitemporal analysis to with the aim of finding and evaluating the scene which spread between the consecutive image acquisition. The applications of this technique can be found in landscape planing, monitoring of global land usage, automatic change detection, monitoring of the tumour evaluation.

Image registration from different viewpoint or viewpoint analysis with the aim of achieving larger 2D view or a 3D representation of the scanned scene applicable in computer vision, remote sensing, shape recovery and so on. Image registration with different sensors or multi-modal analysis. The aim of this method is to integrate the information achieved from various source stream to obtain more complex and detailed scene. This method can be used in medical imaging, radar images independent of cloud cover and solar illumination, remote sensing and so on.

Overaly, image registration plays a significant role in all image analysis tasks that final information is obtained from combination of different data sources, like: multichannel image restoration, image fusion and change detection.

However, the majority of the regularization technique consists of the following steps [5]:

1. Feature detection-Significant and distinctive objects like contours, edges, closed boundary regions can be manually or automatically detected by this technique. For more analysing and processing of these kind of features, they can be shown by their point representative like line ending, center of gravity and distinctive points which are called Central points(CP).

2. Feature matching-In this step the correspondence between feature selected in the original image and those detected in the sensed image is found. Different similarity measures and feature descriptors can be utilized in this part.
3. Transform model estimation-aliasing the scene image with the original image and type and parameters of the so called mapping functions are found in this segmentation step. The mapping function parameters are estimated by means of established feature correspondence.
4. Image sampling and transformation-In this step of segmentation the sensed image is transformed by means of mapping functions.

Using suitable interpolation technique, image value in non-integer coordinate are computed in this part. Figure(2.7) shows 4 aforementioned registration steps.

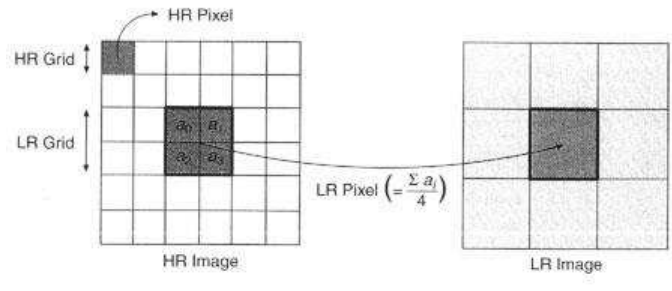


Figure 2.7: 4 steps for registration. First row: Feature detection. Second row: Feature matching by invariant description. Bottom left: Transform model estimation exploiting the established correspondence. Bottom right: Image resampling and transformation. This figure is from [1]

2.3.2 Interpolation

Interpolation is one of the fundamental process in image processing.

Actually, interpolation is the process of estimation the values of a function at position lying between the samples. As a matter of fact, interpolation by fitting a continuous function through the discrete samples can do this. This process authorize input values to be calculated not only at the sample points but also arbitrary.

Interpolation plays opposition role when sampling process generates an infinite bandwidth from a band limited signal due to by applying a low pass filter to the discrete

signal, the bandwidth of the signal decreases. The quality of interpolated image is highly depends on method of interpolation which can be divided into two categories:

1. Deterministic.
2. Statistical interpolation.

Deterministic interpolation

This interpolation technique do under the assumption that there is a high variability between samples. Many different kinds of interpolation can be found in literatures like nearest neighbour, linear and B-Spline. In the following brief description of each of those are presented.

Nearest neighbour

In this approach, interpolated output pixel is allocated to the value of the nearest sample point in the input image which from a computational view point is the simplest interpolation technique. The frequency response of the nearest neighbour kernel can be defined as :

$$H(W) = \text{Sinc}(w/2) \quad (2.2)$$

Kernal and Fourier transform represented in figure(2.8)

Multiplication with a sinc function is equivalent to the convolution in the spatial domain with a rectangle function. Sinc function makes a poor low pass filter due to infinite extension.

This method by using sparse point sampling can obtain minification and by pixel reapplication achieve magnification.

Linear interpolation

By following this interpolation technique which is a first degree it is tried to to passes a straight line through every consecutive point. The frequency response of the linear interpolation kernel is:

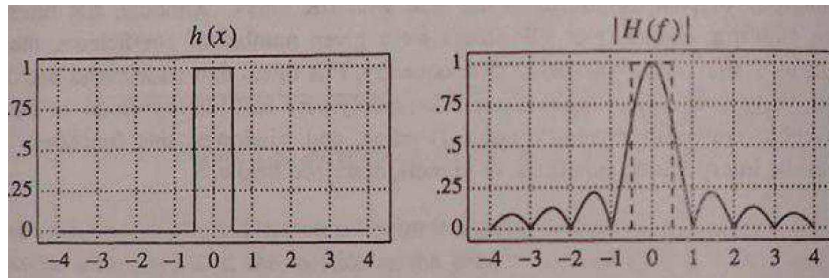


Figure 2.8: Signals in time and frequency domain in nearest neighbour interpolation. This figure is from [11]

$$\mathbf{H}(\mathbf{W}) = \text{Sinc}^2(w/2) \quad (2.3)$$

In comparison with the nearest neighbour interpolation method, performance of this scheme has improved, because the side lobes are less outstanding. Moreover, passband filter is gradually attenuated, resulting in image smoothing. Although the results of linear interpolation is fairly well, but needed for better performance.

Cubic interpolation

This method of interpolation is a third degree interpolation algorithm that its performance is quite well in approximation the theoretical optimum sinc interpolation function.

B-splines

This method of interpolation is derived through n convolutions of the box filters. For example, $B_1 = B_0 * B_0$ represents a B-spline of degree 1 which is equivalent to linear interpolation and $B_2 = B_0 * B_1$ shows the second degree of B-spline and $B_3 = B_0 * B_2 = B_0 * B_0 * B_0$. Figure(2.9) shows the shape of these low order B-splines.

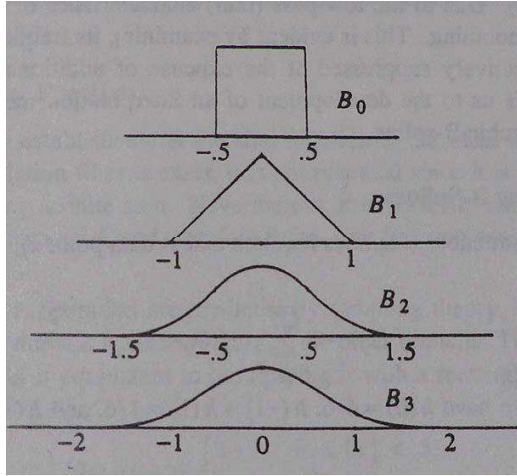


Figure 2.9: Shapes of low order B-splines. This figure is from [11]

This technique of interpolation is an approximating function that passes near the points but not necessarily through them. This method performs well in the image processing applications.

To make a long story short, in our specific super resolution applications, since shift between low resolution images is illegal, images not always match to the high resolution grid, so interpolation should be used.

2.3.3 De-blurring and De-noising

Main aim of super resolution is to achieve a sharp looking high resolution image from a set of low resolution images. Two of the most common difficulties in super resolution concept are noise and blur.

Actually, image reconstruction is an ill-posed problem in the presence of noise [12], while sensors, lens and atmospheric are the reasons of the blur.

Figure (2.10) shows imaging process to be reserved by the super resolution.

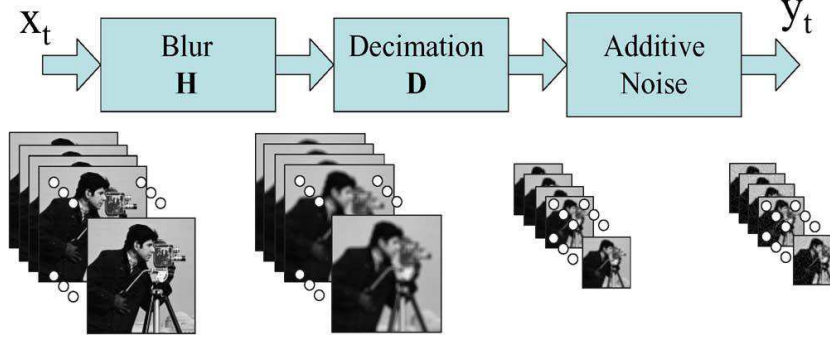


Figure 2.10: Imaging process to be reserved by super resolution. This figure is from [12]

Because of limited resolution that lead to development of up sampling process, image capture process is used for the blurring. Moreover, sub-problem for deblurring natural image is calculating the blur kernel from a single image. Basic methods for denoising, Bayesian and Median filtering, were inclined to remove image details and to over smooth the edges. While, complicated techniques like wavelet based and bilateral filtering use the properties of initial image statistics to strengthen large intensity and decrease lower intensity edges [13].

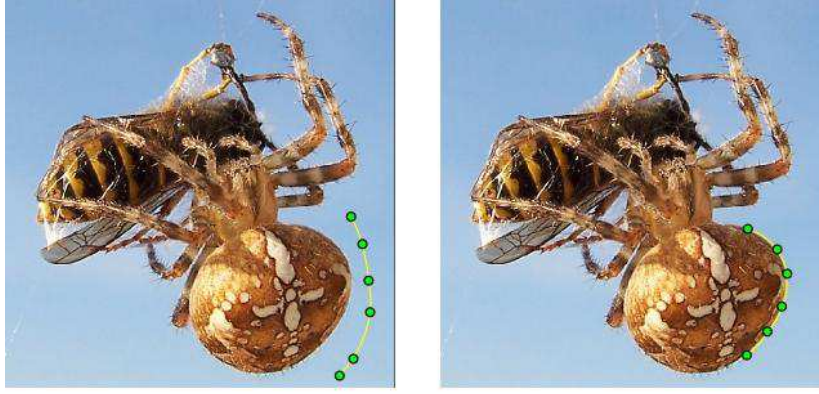


Figure 2.11: Active deformation model. This figure is from wikipedia

2.4 Segmentation

Segmentation scheme is one of the most crucial techniques that is introduced as a useful method for image analysis, understanding and interpretation.

Actually, by using two basic image processing methods, the boundary based (edge-based) segmentation and region-based segmentation, feature-based image segmentation is performed.

2.4.1 Active contour model (Snakes)

Active contour or snake is a structure that defines an object boundary and separates that from possibly noisy 2D image. This outline tries to express energy associated to the current contour as a sum of internal and external energy and make it minimum.

It is worth mentioning that internal energy is minimal when the shape of snake has a high degree of similarity with shape of sought object, considering the shape should be smooth and regular as much as possible. While the external energy of a contour gets its minimum value when snake is at the object boundary.

Active contour models (snakes) could attract attention of scientists due to its possibilities in region grow, edge detection and threshold. Furthermore, this technique is easy to formulate and can achieve sub-pixel accuracy of object boundaries and amalgamation of prior knowledge such as shape and intensity distribution is possible using this technique. Moreover, the result of this process are closed and smooth that can be used for further application such as recognition. Generally, active contour models can be classified into two major groups:

1. Edge based active contour model which uses of image edge information by exploiting image gradient to stop the evolving contours of the object boundaries.
2. Region based methods which without using image gradient tries to identify each region of interest. In this way, this characteristic has made region-based method

less sensitive to image boundaries.

Chen-Vese model is one of the most popular model in this concept. The model using local gradient exploit image information through Mumford-Shah energy functional.

But, unfortunately their model was computationally not enough. Moreover, when level set function be far from a signed distance function their model has the lack of initialization of the level set function.

2.4.2 Model-based active contour

Consider a given valued image $I: \Omega \rightarrow \mathbb{R}^d$ where $\Omega \subset \mathbb{R}^n$, and $d \geq 1$ is the dimension of the vector $I(x)$. Actually, $d=1$ is considered for the gray level images and $d=3$ is considered for the color images. Moreover C is introduced as a closed contour which separates the image domain into outside $C(\Omega_1)$ and inside $C(\Omega_2)$ regions. So, the local intensity fitting energy is defined as:

$$\mathbf{E}_x^{\text{fit}}(\mathbf{C}, \mathbf{f}_1(\mathbf{x}), \mathbf{f}_2(\mathbf{x})) = \sum_{i=1}^{i=2} \lambda_i \int_{\Omega_i} K(x, y) \|I(y) - f_i(x)\|^2 dy \quad (2.4)$$

Where $f_1(x)$ and $f_2(x)$ are two values that approximate intensities in Ω_1 and Ω_2 regions. k as a Gaussian Kernel function is defined as below:

$$\mathbf{k}_\sigma(\mathbf{u}) = \frac{e^{-\|\mathbf{u}\|^2/2\sigma^2}}{(2\pi)^{n/2}\sigma^n} \quad (2.5)$$

It is assumed that the scale parameter $\sigma \geq o$. That is worth mentioning that $k(x - y)$ is effectively zero when $\|x - y\| > 3\sigma$. So, only the intensities in the neighborhood $y: \|x - y\| \leq 3\sigma$ are dominant in the E_x^{fit} and it can be said that E_x^{fit} is localized around the point x . As the intensity $I(y)$ in equation (2.2) can be vary from the entire image domain which corresponds to a large σ centered at x to a small neighborhood which corresponds to a small σ of the point x , it is much more convenient that call E_x^{fit} a Region-Scalable Fitting (RSF) energy. All in all, with given a center point x , the fitting energy E_x^{fit} which is defined as equation (2.4) minimized when the contour C is exactly on the object boundary. In this situation, f_1 and f_2 approximate the image intensities on the both sides of C .

$$\mathbf{E}(\mathbf{C}, \mathbf{f}_1(\mathbf{x}), \mathbf{f}_2(\mathbf{x})) = \int (E_x^{\text{fit}}(C, f_1(x), f_2(x))) dx + \nu \|C\| \quad (2.6)$$

Level set formulation is used to handle it.

In the following basic of "region based level set segmentation method" were presented.

2.4.3 Region based level set for segmentation

In the variational frame, minimization a suitable energy function is introduced for segmentation of the image plane ω . In this way, gradient descent equation is used in

direction of negative energy to evolve the boundary C from some initialization along the normal n with speed function F :

$$\frac{\partial \mathbf{C}}{\partial t} = -\frac{\partial E(C)}{\partial C} = F.n \quad (2.7)$$

A contour is defined as mapping from an interval to the image domain in parametric (explicit) representation (like spline and polygons). A set of ordinary differential equation which acts on the control or marker points is used for implementing the propagation of a parameter contour. Certain regriding mechanisms are introduced to avoid of control system to generate the stability of the contour evolution. For example by introducing by introducing electrostatic repulsion, by impressing in the various formulation a rubber-band like attraction between neighboring points or by numerically resampling the marker point few iterations. Furthermore, to enabling remerging and splitting of the contour, one need to introduce numerical test during the evolution while contours are expressed are expressed as the level line of some embedding function $\phi : \omega \longleftrightarrow R$ in explicit contour representation

$$C = \{x \in \phi \mid \phi(x) = 0\}$$

One method for representing evolve implicitly is using level set technique in which according to a suitable partial differential equation a contour is illustrated by evolving a time dependent embedding function $\phi(x, t)$.

Corresponding partial differential equation might be derieve for the embedding function ϕ for a contour which evolves along the normal n with the speed F a corresponding partial differential equation can be derieved in the following way. The total time derivative of ϕ at locations of the contour must vanish because $\phi(C(t), t) = 0$ for all time.

In this way, we would have :

$$\frac{\partial \phi(\mathbf{C}(t), t)}{\partial t} = \nabla \phi \frac{\partial C}{\partial t} + \frac{\partial \phi}{\partial t} = \nabla \phi F.n + \frac{\partial \phi}{\partial t} = 0 \quad (2.8)$$

Interleaving the definition of the normal $n = \frac{\nabla \phi}{\|\nabla \phi\|}$ then we get the evolution for ϕ :

$$\frac{\partial \phi}{\partial t} = -\|\nabla \phi\| F \quad (2.9)$$

This equation only denote the evolution of ϕ at the location of the contour is obtained. So, the right hand side of equation (2.8) to the image domain away from the contour for the numerical implementation.

In this way, a level set equation can be achieved via variational formulation: Rather than derivating an appropriate partial differential equation for ϕ a variational principle $E(C)$ defined on the space of contours by a variational principle $E(\phi)$ defined on the space of level set function:

$$E_C \longrightarrow E(\phi)$$

so, deriving the Euler-Lagrange equation that minimize $E(\phi)$ is possible :

$$\frac{\partial \phi}{\partial t} = -\frac{\partial E(\phi)}{\partial \phi}$$

As we can see, depending on the choosing embedding, slightly different evolution equation for $\phi(x, t)$ can be obtained. Caselles et.al. and Kichenassamy et.al. proposed independetly a level set formulation for the snake energy as below:

$$\frac{\partial \phi}{\partial t} = \|\nabla \phi\| \text{div}(g(I) \frac{\nabla \phi}{\|\nabla \phi\|}) = g(I) \|\nabla \phi\| \text{div} \frac{\nabla \phi}{\|\nabla \phi\|} + \nabla g(I) \cdot \nabla \phi \quad (2.10)$$

As equation (2.10) denoted the length of the contour in Riemannian space, this approach is known as Geodisic Active Contour.

Snakes as an optimization technique have been evaluated because algorithms are easily trapped in local minima which are not suitable. In this way, the result of segmentation is highly dependent on initialization. Actually, in the presence of noise local maxima of the image gradient produce many local minima. So additional balloon force is introduced to expresssion of the contour toward the object's boundaries of interest. In the following, we will review a probabilistic formulation of the problem of segmentation.

Two-phase level set formulation

In this method, each pixel in the domain Ω is assigned to one of two areas: inside and outside the contour. To do this, (2.16) is extended using Chan and Vese approach [34], and can be achieved :

$$\mathbf{E}(\phi, \theta_i) = - \int_{\Omega} H(\phi) \log p(f|\theta_1) - (1 - H(\phi)) \log p(f|\theta_2) + \nu \|\nabla H(\phi)\| dx \quad (2.11)$$

$H(\phi)$ as would be mentioned in the following, is the Heaviside function. The first two terms in equation (2.19) represents inside and outside the contour, while the last term shows the length of separating interface. Gradient descent is used for the embedding function ϕ for minimization:

$$\frac{\partial \phi}{\partial t} = \delta(\phi) \nu \text{div} \frac{\nabla \phi}{\|\nabla \phi\|} + \log \frac{p(f(x)|\theta_2)}{p(f(x)|\theta_1)} \quad (2.12)$$

It is worth mentioning that θ_i should be updated according to (2.18).

2.4.4 Multiphase level set formulation

Finding a way to handle a larger number of phases attract the attention of many researchers in recent years. As most of these proposed techniques assigned a separate level set function to each region, computation complexity increase. Furthermore, because of suppressing of vacume or overlap regions numerical implementation is something involved.. Chan and Vese derived a fantastic formulation by interpreting these overlap regions as separate regions. Following their formulation n regions can be modeled. Actually, their technique only require \log_2^n level set function.

2.4.5 Image segmentation as Bayesian inference

In fact, from the Minimum Description Length (MDL) criterion, a segmentation functional can be achieved, and by maximizing the a posteriori probability $p(P(\Omega)|I)$ for an given image I a optimal partition $p(\Omega)$ of the image plane Ω can be calculated. According to Bayes rule we would have:

$$\mathbf{p}(\mathbf{P}(\Omega)|\mathbf{I}) \propto p(I|P(\Omega))p(P(\Omega)) \quad (2.13)$$

Bayesian framework is widely used in computer vision to trackle many ill-posed problems. The reasons for this probability is as follows:

1) The term $p(P(\Omega))$ in (2.11) allows us to have some prediction about which represents interpretation of the data are a priori more or less likely which can be used to manage with missing low level information.

2) The conditional property $p(I|P(\Omega))$ given a model state is usually easier to model than the posteriori distribution.

The most commonly used regularization constraint

$$\mathbf{p}(\mathbf{P}(\Omega)) \propto \exp^{\nu\|C\|} \quad (2.14)$$

Which is a priori that support along the short length C of the boundary of image.

With the assumption that of having no correlation between the labling it is assumed that the image partition to be composed of N regions which lead us to the following:

$$\mathbf{p}(\mathbf{I}|\mathbf{P}(\Omega)) = p(I|\Omega_1, \Omega_2, \dots, \Omega_N) = \prod_i^N p(I|\Omega_i) \quad (2.15)$$

In the above formulation $p(I|\Omega_i)$ represents the probability of observing image I with the assumption of Ω_i is the region of interest.

It assumed that associated with each image location, regions are characterized by a given feature $f(x)$, which this figure can be colour or the spacio-temporal image gradient. Moreover, it is considered that the numerical values of f modeled as identically distributed realization and are identical pertinent to the same random process. With the assumption of P_i be a probability density function of that random process in Ω_i , equation (2.13) reads

$$\mathbf{p}(\mathbf{I}|\mathbf{P}(\Omega)) = \prod_i^N \prod_{x \in \Omega_i} (p_i(f(x)))^{dx} \quad (2.16)$$

Where dx is used to be sure about the correct continuum limit equation (2.14) is not generally valid because image feature denote local spatial correlations. Minimizing the equation (2.11) is equivalent to maximizing a posteriori probability. So, we can end up with the following:

$$\mathbf{E}(\Omega_1, \dots, \Omega_N) = - \sum_i \int_{\Omega_i} \log p_i(f(x)) dx + \nu\|C\| \quad (2.17)$$

Above equation is achieved by integrating the regularity constraint (2.12) and the region-based image term. Actually, calculating this amount of energy is the basis of broad range of works. So, it is worth mentioning that the region statistics can be computed interweaved with the estimation of boundary C.also, appropriate intensity histograms can be computed.

Distribution can be estimated either parametric or non-parametric. This energy takes the form of equation(2.16)if parametric representation with the parameter θ_i is used.

$$\mathbf{E}(\Omega_i, \theta_i)_{i=1,2,\dots,N} = - \sum_i \int_{\Omega_i} \log p(f(x)|\theta_i) dx + \nu \|C\| \quad (2.18)$$

The optimal parameters can be defined as follows:

$$\mathbf{E}(\Omega_i)_{\mathbf{i}} = \min E(\Omega_i, \theta_i) = \sum_i \int_{\Omega_i} \log p(f(x)|\theta_i) dx + \nu \|C\| \quad (2.19)$$

And

$$\theta_i = \operatorname{argmin}_{\theta} (- \int \log p(f(x)|\theta) dx) \quad (2.20)$$

In this case, the optimal model parameters θ_i is completely depends on the regions Ω_i . This dependency to regions is so crucial in calculating of exact shape gradients, which can be applied in non-parametric density estimation scheme.

Scalar image

In scalar image it is assumed that the intensities can be obtained from Gaussian distribution moreover, each image is made of two regions. So :

$$\mathbf{p}(\mathbf{I}|\mu_i, \sigma_i^2) = \frac{\exp \frac{-(I-\mu_i)^2}{2\sigma_i^2}}{\sqrt{2\pi\sigma_i^2}} \quad (2.21)$$

Where $i = 1, 2$

Belows you can find the optimal values for the mean μ_i and the variance σ_i that can be achieved analytically:

$$\mu_1 = \frac{1}{\sigma_1^2} \int H(\phi) I(x) dx \text{ and } \sigma_1^2 = \frac{1}{a_1} \int H(\phi) (I(x) - \mu_1)^2 dx$$

$$\mu_2 = \frac{1}{\sigma_2^2} \int (1 - H(\phi)) I(x) dx \text{ and } \sigma_2^2 = \frac{1}{a_2} \int (1 - H(\phi)) (I(x) - \mu_2)^2 dx$$

where $a_1 = \int H(\phi) dx$ and $a_2 = \int (1 - H(\phi)) dx$ that denoted that the areas of inside and outside regions.

Using gradient descent for the level set function ϕ leads:

$$\frac{\partial \phi}{\partial \mathbf{t}} = \delta(\phi) (\nu \operatorname{div} \frac{\nabla \phi}{\|\nabla \phi\|} + \frac{(I - \mu_2)^2}{2\sigma_2^2} - \frac{(I - \mu_1)^2}{2\sigma_1^2} + \log \frac{\sigma_1}{\sigma_2}) \quad (2.22)$$

That is worth mentioning that level set evolution iteration is only calculated inside a narrowband around the zero crossing, because the delta function is equal to zero at other locations. Moreover, the updated values depends on the previous values and location of changing the sign of ϕ for each pixel.

Vector valued images

By using this technique, the 2-phase segmentation of an image can be achieved as below:

$$\frac{\partial \phi}{\partial \mathbf{t}} = \delta(\phi) (\nu \operatorname{div} \frac{\nabla \phi}{\|\nabla \phi\|} + \log \frac{p(I(x)|\mu_2, \sum_2^2)}{p(I(x)|\mu_1, \sum_1^2)}) \quad (2.23)$$

Where $\mu_1 = \frac{1}{\|\Omega_i\|} \int_{\Omega_i} I(x)$ and $\sum_i = \frac{1}{\|\Omega_i\|} \int_{\Omega_i} (I(x) - \mu_i)(I(x) - \mu_i)^T$ for $i=1,2$

Similar to the case of scalar image, to keep away from a full computation over the whole image domain, the evaluation of the statistical parameters can be optimized.

As mentioned before, level set is a numerical technique for tracking interfaces and shapes. The most crucial advantage of level set is that following shapes that change topology is become easy.

Moreover, without having parameter curves and surfaces one can perform numerical computation[19].

In level set formulation, a contour $C \subset \Omega$ is signified by the zero level set of a Lipschitz function:

$$\phi: \Omega \rightarrow \mathbb{R}.$$

It is assumed that ϕ takes positive values inside the contour while, negative values outside the contour C . The energy functional $E_x^{fit}(C, f_1(x), f_2(x))$ can be defined as below:

$$\mathbf{E}_\xi(\phi, \mathbf{f}_1, \mathbf{f}_2) = \sum_{i=1}^2 \lambda_i \int \left(\int k_\sigma(x-y) \|I(y) - f_i(x)\|^2 M_i^\xi(\phi(y)) dy \right) dx + \xi \int \|\nabla H_\xi(\phi(x))\| dx \quad (2.24)$$

Which $M_1(\phi) = H(\phi)$ and $M_2(\phi) = 1 - H(\phi)$ and H is Heaviside function which is a non-continuous function whose value is zero for negative argument and one for positive argument. It is the matter of importance that the Heaviside function can be approximated by a smooth function:

$$\mathbf{H}_\xi(\mathbf{x}) = \frac{1}{2} \left[1 + \frac{2}{\pi} \arctan\left(\frac{x}{\xi}\right) \right] \quad (2.25)$$

The level set regularization term is defined as below:

$$\mathbf{P}(\phi) = \int \frac{1}{2} (\|\nabla \phi(x)\| - 1)^2 dx \quad (2.26)$$

This factor plays a pivotal role in the level set concept because without this term contour motion becomes very slow and before it can reaches to the preferred object

boundaries can be stopped. Furthermore, this function describes the variation of the function ϕ from a signed distance function. That is proposed to minimize the energy functional with respect to functions f_1 and f_2 with a fixed level set function:

$$\mathbf{F}(\phi, \mathbf{f}_1, \mathbf{f}_2) = E_\xi(\phi, f_1, f_2) + \mu P(\phi) \quad (2.27)$$

Where μ is a positive constant. To minimize the energy functional, gradient descent technique which is an first order optimization to find a minimum of a function is utilized which leading to the following formula:

$$\mathbf{f}_i(\mathbf{x}) = \frac{k_\sigma(x)[M_i^\xi(\phi(x))I(x)]}{k_\sigma(x) * M_i^\xi(\phi(x))} \quad (2.28)$$

With keeping f_1 and f_2 fixed by solving the gradient flow equation, it is possible to define the the energy function and try to minimize it:

$$\frac{\partial \phi}{\partial t} = -\sigma_\xi(\phi)(\lambda_1 e_1 - \lambda_2 e_2) + \nu \sigma_\xi(\phi) \operatorname{div}\left(\frac{\nabla \phi}{\|\nabla \phi\|}\right) + \mu(\nabla^2 \phi - \operatorname{div}\left(\frac{\nabla \phi}{\|\nabla \phi\|}\right)) \quad (2.29)$$

The first term in equation(2.10) is referred as the Data Fitting Term because this item is responsible for the driving active contour toward the object boundary. Actually, the effect of this item should not be ignored.

The second term is Arc Length Term which has a smoothing effect on the zero level cotour.

And finally, the third term as mentiond earlier is the Level Set Regularization Term.

2.4.6 Level set method and image segmentation

For detect objects in an image u_0 , the active contour(snake)model evolves a contour $\Gamma(t)$. The curve is moved in the direction normal to the curve from an initial position. When $\Gamma(t)$ is placed at the boundary of an image is explicit via an edge detection function

One limitation of the original snake model is the explicit representation of the curve, so merging and breaking and other topological changes, are not easy to handle in this way, the level set for active contour model segmentation was introduced [14].

The curve evolution is based on general Mamford-Shah formulation of image segmentation minimization of below function:

$$= \int_{\omega/T} \|u - u_0\|^2 dx + \beta \|T\| + \nu \int_{\omega/T} \|\nabla u\|^2 dx \quad (2.30)$$

Where $\|T\|$ represent the length of Γ . A minimizer of this function in ω/T is smooth.

It is worth mentioning that the last two terms of above equation measuring curve length of the curve bounding the phase and make u smooth in ω/T .

Furthermore, the amount of smoothness and regularization can be control by β and ν .

Moreover, following minimization problem are proposed for 2-phase segmentation:

$$\min \left[\int_{\Omega} \|\mathbf{u}_0 - \mathbf{c}_1\|^2 \mathbf{H}(\phi) d\mathbf{x} + \int_{\Omega} \|\mathbf{u}_0 - \mathbf{c}_2\|^2 (1 - \mathbf{H}(\phi)) d\mathbf{x} + \nu \int_{\Omega} \mathbf{H}(\phi) d\mathbf{x} + \beta \int_{\Omega} \delta(\phi) \|\nabla \phi\| d\mathbf{x} \right] \quad (2.31)$$

Where ϕ is the level set function, $H(\phi)$ as mentioned before, is heaviside function. By moving ϕ in the steepest descent direction and by introducing an artificial time variable, the minimum of above equation can be found as below:

$$\phi_t = \delta_{\varepsilon}(\phi) (-(u_0 - c_1)^2 + (u_0 - c_2)^2 - \nu + \beta \nabla \left(\frac{\nabla \phi}{\|\nabla \phi\|} \right)) \quad (2.32)$$

$\phi(t_0) = \phi_0$ It is worth mentioning that the recovered image is a piecewise constant approximation to u_0 .

3

Softwares

In this chapter some information of softwares that are used in this master thesis are presented.

Two software packages are downloaded and used in this thesis :

1. Super resolution image reconstruction software package by the website software downloaded from:

[//lcav.epfl.ch/software/superresolution](http://lcav.epfl.ch/software/superresolution)

and download Matlab code: superresolution.v2.0.zip(128 Kb).

2. The level set segmentation by the waebite downloaded from:

<https://sites.google.com/site/clictoolkit/image-segmentation/region-based-model>

and downloaded Matlab code:

[http : //www.engr.uconn.edu/ cmli/code/RSF_v0_v0.1.rar](http://www.engr.uconn.edu/~cmli/code/RSF_v0_v0.1.rar)

3.1 SR image reconstruction Software

Super resolution as mentioned earlier, is the process of combining some low resolution images to achieve a high resolution image. This process also has a pivotal role in reducing aliasing[6].

Vandewalle et.al. developed a collection of methods, including non-uniform interpolation using Delaunay triangulation.

So, it is useful to have a brief review and understanding about super resolution software which is widely used in producing super resolution images[6].

This software enables users to compare different method of super resolution that exist today. Starting with this software simply done by typing 'superresolution' in the MATLAB console. So, a window appear which including several parts as below:

Source image: Loading a set of low resolution images is done in this part. user can using low resolution images that he has or either can use the capability of this software to produce a set of low resolution images from an initial high resolution. In both cases 'Add' button on the left side of the screen should be clicked.

Moreover, user can remove any selected image from the list by selecting that and clicking on the 'Remove' button.

Furthermore, removing all images can be done by selecting all images and clicking 'Remove all images'. Meanwhile, software ask user to where save generated low resolution images.

After loading low resolution images, that is time to do motion estimation and selecting the reconstructing technique.

Motion estimation: For the motion estimation, user may be asked to estimate whether by the shifts or both shifts and the rotations or it may be asked to multiply each low resolution image with a Turkey window which will add a slightly disappearing back border to it.

It is a matter of importance that motion parameters can be entered manually. In this case user is asked about the location and number of the low resolution images and then user should indicate the parameters like: rotation shift(that should be in Radian), shifting along X direction and shifting along Y axis.

For the reconstruction techniques, user may indicate the interpolation factor and the percentage of the image that he wants to be processed. Actually,in whole of the images that processed in this work, interpolation factor was considered as 4 and full image reconstruction has been used.

Finally, user is asked where is his favourite location to save the result image or software save it in the current directory.

The format of the image achieved in result is .TIF, in order to avoid any unwanted compression artifact.

3.1.1 Motion Estimation Algorithms

The algorithms which has been used in this software for estimating the motion are as below:

Vandewalle et al. Algorithm [6]

This method is based on the fact that a shift in the space domain is translated into a linear shift in the phase of the Fourier Transform of the image. Likewise, a rotation in the space domain is visible in the amplitude of the Fourier Transform.

Actually, in this method instead of using whole frequency spectrum only parts of frequency spectrum is considered that the signal to noise ratio is highest and aliasing is minimal. So, this algorithm is not able to reconstruct a better image as the method uses exactly this under sampled information.

Although, one advantage of using this algorithm is that high frequency components, where aliasing may have occurred is discarded.

In fact, this method is suitable with slight camera motion condition or satellite images. The performance of this method surpasses many other frequency algorithm and directive spatial algorithm in terms of SNR and subjective quality.

Marcel et al. Algorithm [6]

Likewise Vandewalle algorithm, frequency domain has been used in this technique, to determine the shift and frequency.

In fact, Nearly all of the frequency domain registration are based on the fact that two shifted images correspond to the phase shifted in the frequency domain.

Therefore by utilizing Log-Polar transform of the magnitude of the frequency domain, rotation and scale of the image can be adopted into horizontal and vertical shifts.

Actually, in this algorithm Fourier domain image was transformed into a shift.

Lucchese and cortelazzo Algorithm [6],[15]

Their scheme is based on the fact that the image Fourier Transform magnitude and the mirrored version Fourier Transform of the rotated image would have a zero-crossing lines.

The angle between two images can be find easily by angle that these zero-crossing lines makes with the axis,

Karen et al. Algorithm [6]

The motion estimation algorithm by Karen et al. is so efficient and straightforward.

This algorithm uses different down-sampled versions of the specific image. At first, it uses from a down sampled image by a factor 4 to do the estimation of the shift and rotation via Taylor series.

After the correction for the shifts and estimation of the rotation has been done, the image should be down sampled by the factor 2.

Finally, the same is done with the full resolution image, in order to fine-tune the estimation.

As a mater of fact, this method is applied on a series of images taken from a moving camera. This method is beneficial for set of images that taken from an aircraft or satellite where they are differ mostly rotation and translation. Actually, Karen realized recursive iteration super resolution method to minimize errors between low resolution images.

3.1.2 Reconstruction Algorithm

Super resolution reconstruction is a well known problem and extensively treated in the literatures. Main aim of this concept is to recovery a single high resolution image from a series of low quality images.

Generally speaking, the super resolution problem may consist of imaging with space variant blur, geometric warp and color noise.

There are several algorithms that already proposed dealing with such a problem. In the following we have a brief review of reconstruction algorithms in the aforementioned software.

Interpolation Algorithm

The software simply aligns all the pixel of the image on a high resolution grid and then using Mat Lab's built-in `griddata` function, applies a bicubic interpolation.

Papoulis-Gerchberg Algorithm [16],[6]

This technique is a kind of POCS(Projection Onto Convex Sets) method that cuts the high frequencies by situating the given pixels on a high resolution grid goes into the frequency domain, and we can say that it is assumed that the missing data correspond to a missing region in the frequency domain. This method can only applies to a parallel beam scanning geometry that makes this scheme restrictive. Moreover, where rather than complete projection, arbitrary line integrals are missing, the frequency domain approach does not even apply to a parallel beam geometry. This process continues until convergence.

Iterated Back Projection Algorithm [17]

The idea behind iterated back projection reconstruction technique is estimation of high resolution image and then iteratively add it to the sum of errors between each low resolution image and the estimated high resolution image that went through suitable transforms that is given by motion estimations.

Estimation is based on too many assumptions like motion model and noise. The estimation is not considered to be exactly true but, they are suitable mathematical information based on some prior information [18].

Robust Super Resolution Algorithm [19]

Robust super resolution is far more robust version of the above iterated back projection.

The only difference resides in the computation of the gradient, which is not given by the sum of all errors,. But, by median of all errors.

This brings robustness against outliers in the low resolution images.

Projection Onto Convex Sets(POCS) Algorithm [20]

In fact, this method describes an alternative approach to incorporating prior knowledge about the solution into the reconstruction process.

Actually, this technique is so similar to to Papoulis-Gerchberg method. But, instead of cutting the high frequency the image is passing through a low pass filter. This filter estimate the power spectrum function of the camera.

Moreover, the advantage of this technique is its simplicity that utilizes the powerful special domain observation and it allows a convenient inclusion of priori information. But, its disadvantage is its slow convergence and high computational cost. It is worth mentioning that, noise don't take into account in this method.

Structure-Adaptive Normalized Convolution Algorithm [21]

This method is based on the Normalised Convolution(NC) structure.

In this approach local signal is estimated through projection onto a subspace.

Normal convolution is equivalent to local series expansion if polynomial basis function is used.

This algorithm use two options to crate high resolution image from set of low resolution as below:

- A second pass can be implemented in the correction, which will accept the orientation and the size of Gaussian filters that used in normal correlation. This process would result a sharper high resolution image.
- Noise robustness will analyse the images and find out which pixels are noisy to not to use them.

The Graphical User interface looks as below:

Below figure depicts what we face when run super resolution software.

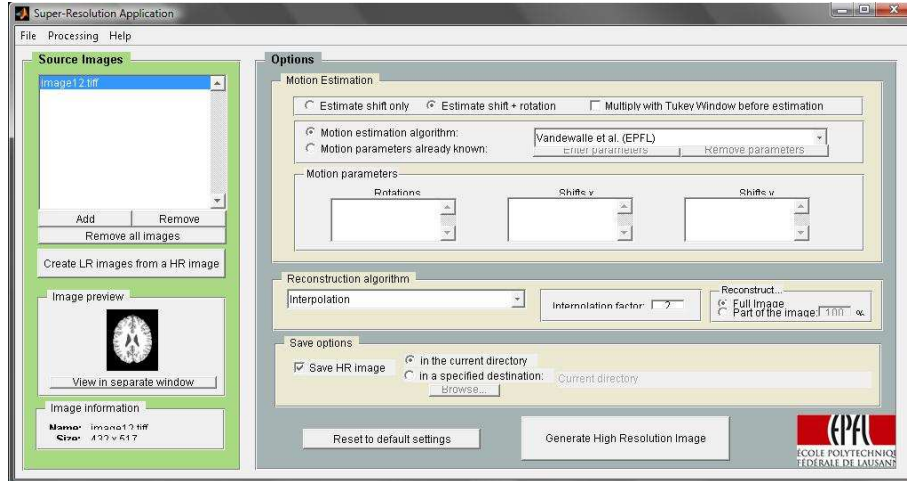


Figure 3.1: Super Resolution Software. This figure is a result of running the software that can be found in [//lcam.epfl.ch/software/superresolution](http://lcam.epfl.ch/software/superresolution)

3.2 Level set segmentation software

The software that are explained below, was proposed by Chunming Li in 2008 [22], and software can be found in [22].

This software is based on the "Region Scalable Fitting Energy" that explained in previous chapter. The variety of parameters that used in this software in terms of application gets different values. Here the parameters are set according to MR image as below:

Iteration number=400

σ (scale parameter)=3

$\lambda_1=1$

$\lambda_2=2$

time step=0.1

$\mu=1$

$\nu = 0.003 \times 255 \times 255$

Actually, the number of iteration depends on the location of initial contour. This factor does not have any significant influences on the resultant image.

Also, larger scale parameter is corresponds to dependency of the location of the initial contour while smaller value of scale parameter is corresponds to more exact location of the object boundaries. The image (3.2) and (3.3) shows the segmentation results for two scale parameter 4 and 10.

The Segmentated Image with scale parameter=4

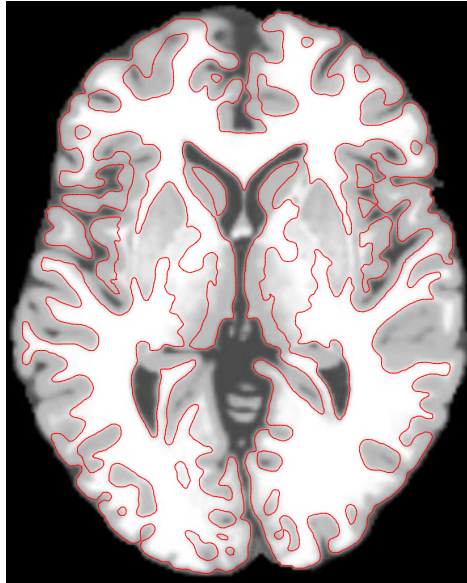
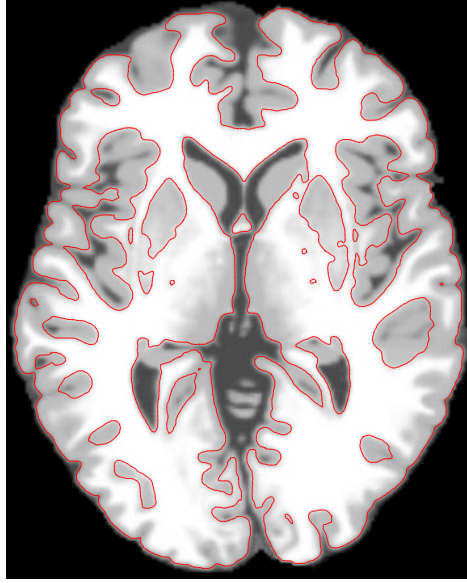


Figure 3.2: Scale parameter=4

The Segmented Image with scale parameter=10

**Figure 3.3:** Scale parameter=10

Here, two values of 2 and 1 are chosen for two parameters λ_1 and λ_2 to avoid the emergence of new contour far away from the initial contour such as skull.

In fact, when different values of λ_1 and λ_2 are used, the amount of reprimand that imposed on the integrals inside and outside the contour is different, while equality of λ_1 and λ_2 demonstrates that a fair competition between inside and outside of the boundary during the evolution.

Moreover, to further penalty the contour length that also deject the expansion of the contour to some extend, larger value compared to other experiments is chosen for ν for our specific usage, MR image.

it is worth mentioning that interior boundaries can be detected because of the emergence of the new counters that is the main aim of fast evolution of curve toward final results.

The data fitting term $-\delta_\epsilon(\lambda_1 e_1 - \lambda_2 e_2)$ in (2.29) has significant role on the change of ϕ in the whole image domain. In this way, emergency of new contour is doubled.

Moreover, $(\lambda_1 e_1 - \lambda_2 e_2)$ has a large value for point x that is close to object boundary but, they are far away from the zero level set contour.

Furthermore, the data fitting term $\delta_\epsilon(\lambda_1 e_1 - \lambda_2 e_2)$ is not zero and should not be over looked; because $\lambda_\epsilon(\phi)$ takes small values far away from zero level set.

All in all, at strong object boundary new zero level contour may change. Particularly in most occasion like binary step function when level set function ϕ is initialized to be

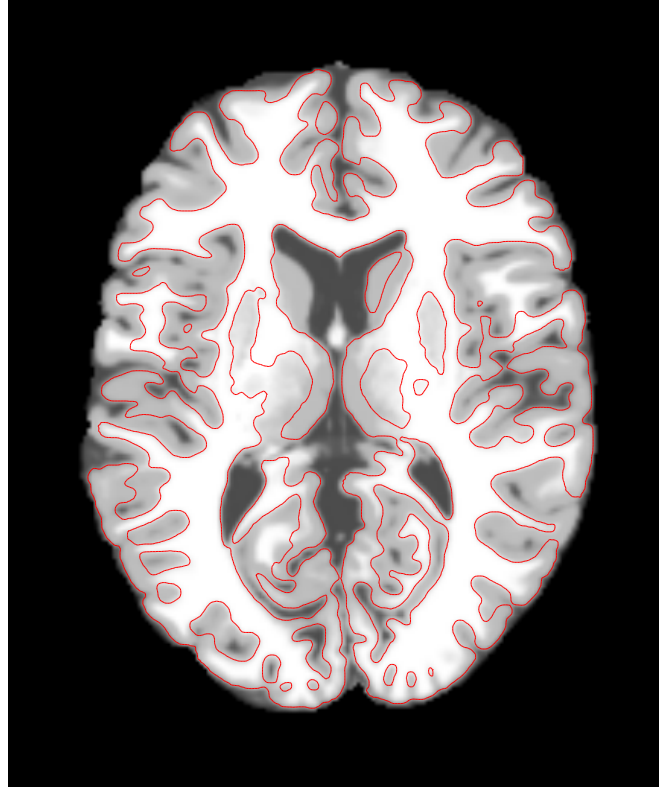


Figure 3.4: Segmentation result with: Iteration number=500, $\lambda_1=1, \lambda_2$, time step=0.1, $\mu=1, \nu=0.003 \times 255 \times 255$ and $\delta=3$

small values.

Generally speaking, selecting larger values of ϵ a broader value of δ_σ is accessible that pave the road of easy emerge of new contour. On the other side of the coin, broader profile of σ_ϵ make the accuracy in the final contour location less accurate.

Figure (3.4) shows segmentation result for MR image with the aforementioned parameter.

Figure (3.3) shows segmentation result fore MR image with the aforementioned parameter.

4

Testing a super-resolution image segmentation method

This thesis suggests a method to improve segmentation scheme by combination of super resolution with one of the segmentation technique which is known as level set segmentation technique.

To the author's knowledge this combination has not been used so far. Along this technique, firstly the super resolution is applied on images and then ,as be can seen in image below, SR images are processed with level set segmentation technique.

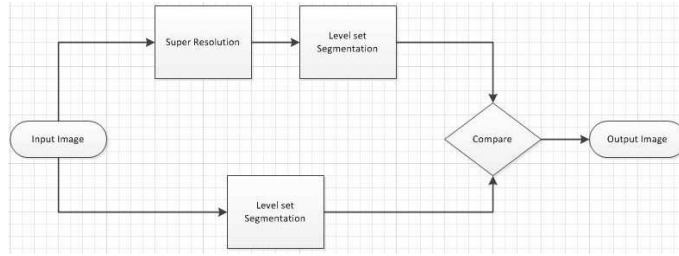


Figure 4.1: Proposed technique

Next time images were applied directly to segmentation process.

The result show that the combination of super resolution and level set segmentation technique have better results.

it is a matter of importance that different parameters can be applied to each super resolution and level set segmentation scheme each has specific result that can be seen in chapter 5.

5

Experiment results

Experiments were conducted to compare between segmentation of high resolution images and low resolution images.

5.1 Segmentation evaluation

In segmentation evaluation part, we first partitioned images into image segments and then do analysing based on texture, shape or spectral features.

There are so many types of algorithms in image segmentation which each of them developed for a variety of applications from remote sensing image analysis to medical imaging.

In this way, having a benchmark for deciding which of them can perform better is highly demanded.

Actually, such as segmentation, there is no standard way for evaluation of segmentation.

As a matter of fact, segmentation evaluation is completely subjective and serious problem in the field of image analysis.

In some circumstances, the concept of evaluation of segmentation is based on how well the segmented image corresponds to the ground truth segmentation based on pixel by pixel differences.

But, there is no unique ground truth of segmentation for images. However, if a specific model of ground truth is selected, in almost all applications of scene analysis, the difference between segmented image and ground truth should be minimized.

Hence, the criterion of segmentation are rather harsh in terms of penalizing algorithms severely if they don't segment accurately.

On the other side, in some applications for instance, medical imaging overlapping of segmented image with the true region would be sufficient.

Hence, if segmentation only partially detects the true region or border can be considered acceptable.

The evaluation of image segmentation that is an essential field of study, is classified into 2 groups and this classification is based on whether a priori information is available or not. These 2 groups are: Supervised and Unsupervised image segmentation.

A broad range of approaches have been proposed that quantitative technique is one of them.

Rosefed and Weskafor, measured and categorized error by using busyness measure. Lavine and Nazif [23] focused on unsupervised segmentation and define parameters like region contrast and region uniformity and line contrast.

Soha et al. used of some parameters that defined by Zarif and Lavine such as uniformity criterion to compute shape measure. Actually, these computation was based on gradient values and selected threshold value. Error are measured using a reference in the case of supervised segmentation.

The difference between segmentation output and reference image is that how well the algorithm of segmentation performs.

The simplest scheme that is used for supervised segmentation ought to be probability of errors that can be used for finding optimal threshold values. However, this error can't give any information about image quality.

Another, approach for measuring the segmentation quality is calculating the difference between the actual segmented image and ideally segmented image. It is worth mentioning that these can be any object feature [24].

5.2 Experimental set-up

The segmentation package parameters setting is as follow:

- Iteration number: Defines the number of iterations, that depends on the location of of initial contour.

- Scale parameter: Controls the size of image intensities in a region. This value corresponds to scale parameter in Gaussian-Kernel that set to 1.

- Time step: The value of this parameter is set to 0.1

Furthermore, the Super resolution setting can be found in each example separately.

That is worth mentioning that Super resolution and Segmentation packages have better results for aforementioned settings.

5.3 Experiment results

In the following some segmentation results in both low resolution and super resolution images can be found and compare.

Most of the images that have been segmented in this part are from Berkeley Segmentation Dataset.

5.3.1 Example 1

The parameters that applied on Super resolution software are as below:

The number of low resolution images:10

The super resolution and Low resolution Image size: 248×248

The interpolation factor:2

The motion estimation method: Vandewalle et al.

The reconstruction method:Interpolation

The interpolation factor:2

Furthermore the motion parameters are considered as below:

Rotation:

$R_1 = 0; R_2 = 0; R_3 = -0.1; R_4 = 0; R_5 = 0; R_6 = 0; R_7 = 0; R_8 = -0.1; R_9 = 0; R_{10} = 0$

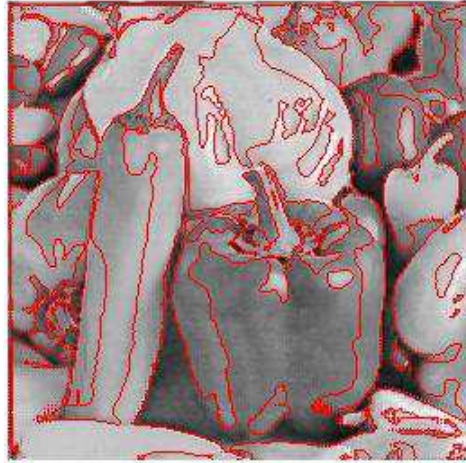
Shift in x direction:

$t_{x1} = 0.0; t_{x2} = 0.1635; t_{x3} = 0.2776; t_{x4} = 0.0360; t_{x5} = 0.0930; t_{x6} = 0.790; t_{x7} = 0.6382; t_{x8} = 0.2961; t_{x9} = 0.8515; t_{x10} = 0.0181$

Shift in y direction:

$t_{y1} = 0.0; t_{y2} = 0.4435; t_{y3} = 0.7651; t_{y4} = 0.8196; t_{y5} = 0.1731; t_{y6} = 0.5332; t_{y7} = 0.5034; t_{y8} = 0.6543; t_{y9} = 0.7569; t_{y10} = 0.7805$

Segmentation of super resolution image with RSF method(2008)



Iterations=1500,time step=0.10,mu=1,epsilon=.9,sigma=2.00,lambda1=1,lambda2=1

Segmentation of low resolution image with RSF method(2008)



Iterations=1500,time step=0.10,mu=1,epsilon=.9,sigma=2.00,lambda1=1,lambda2=1

Figure 5.1: Segmentation of high resolution image (Up) and low resolution image(Down)

5.3.2 Example 2

The super resolution and Low resolution Image size: 237×157

The motion parameters are considered as below:

Radiation:

$R_1 = 0.0; R_2 = -0.1; R_3 = -0.1; R_4 = 0.0; R_5 = 0.0; R_6 = 0.0; R_7 = 0.0; R_8 = 0.0; R_9 = -0.1, R_{10} = 0.0$.

Shift in the X direction:

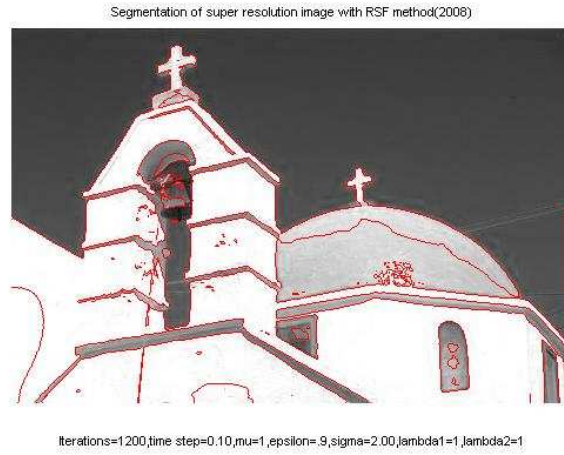
$t_{x1} = 0.0; t_{x2} = 0.04233; t_{x3} = 0.4332; t_{x4} = 0.5054; t_{x5} = 0.9550; t_{x6} = 0.0890; t_{x7} = 0.4160; t_{x8} = 0.3442; t_{x9} = 0.0732; t_{x10} = 0.284$

Shift in y direction:

$t_{y1} = 0.0; t_{y2} = 0.7215; t_{y3} = 0.2293; t_{y4} = 0.2490; t_{y5} = 0.0463; t_{y6} = 0.2993; t_{y7} = 0.1196; t_{y8} = 0.3196; t_{y9} = 0.6175; t_{y10} = 0.5349$

Other parameters remain the same as previous example.

Figures(5.3) and (5.4) show the segmentation results of super resolution and low resolution images.



Segmentation of low resolution image with RSF method(2008)



Iterations=300,time step=0.10,mu=1,epsilon=.9,sigma=2.00,lambd1=1,lambd2=1

Figure 5.2: Segmentation of high resolution image (Up) and low resolution image(Down)

5.3.3 Example 3

The super resolution and Low resolution Image size: 286×218

The motion parameters are considered as below:

Radiation:

All radiation parameters are set to zero.

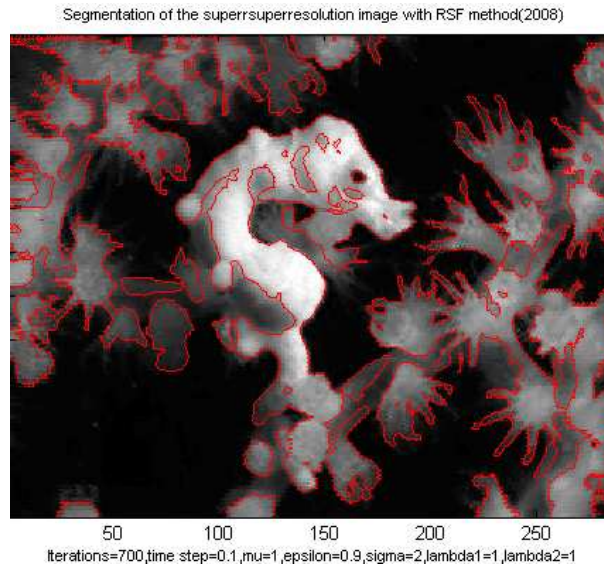
Shift in x direction:

$t_{x1} = 0.0; t_{x2} = 0.20; t_{x3} = 0.73; t_{x4} = 0.83; t_{x5} = 0.47; t_{x6} = 0.15; t_{x7} = 0.30; t_{x8} = 0.44; t_{x9} = 0.52; t_{x10} = 0.29$

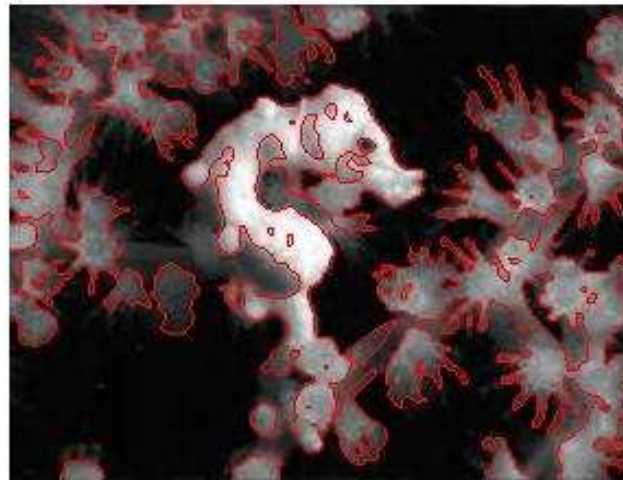
Shift in y direction:

$t_{y1} = 0.0; t_{y2} = 0.68; t_{y3} = 0.25; t_{y4} = 0.018; t_{y5} = 0.26; t_{y6} = 0.25; t_{y7} = 0.40; t_{y8} = 0.45; t_{y9} = 0.08; t_{y10} = 0.22$

Other parameters remain unchanged, following images depicts the results of super resolution and low resolution segmentation images.



Segmentation of low resolution image with RSF method(2008)



Iterations=700,time step=0.10,mu=1,epsilon=.9,sigma=2.00,lambda1=1,lambda2=1

Figure 5.3: Segmentation of high resolution image (Up) and low resolution image(Down)

5.3.4 Example 4

The super resolution and Low resolution Image size: 238×157

The motion parameters are considered as below:

Radiation:

$R_1 = 0.0; R_2 = -0.1; R_3 = -0.1; R_4 = -0.1; R_5 = -0.1; R_6 = -0.1; R_7 = -0.1; R_8 = -0.1; R_9 = -0.1; R_{10} = -0.1$.

Shift in x direction:

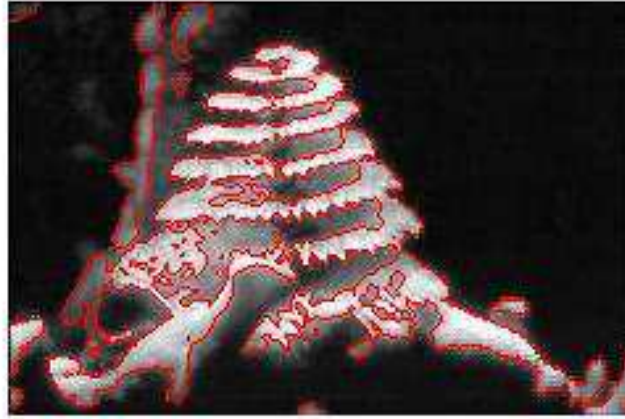
$t_{x1} = 0.0; t_{x2} = 0.82; t_{x3} = 0.01; t_{x4} = 0.61; t_{x5} = 0.47; t_{x6} = 0.01; t_{x7} = 0.135; t_{x8} = 0.41; t_{x9} = 0.71; t_{x10} = 0.86$

Shift in y direction:

$t_{y1} = 0.0; t_{y2} = 0.81; t_{y3} = 0.58; t_{y4} = 0.09; t_{y5} = 0.44; t_{y6} = -0.1; t_{y7} = 0.085; t_{y8} = 0.64; t_{y9} = 0.39; t_{y10} = 0.80$

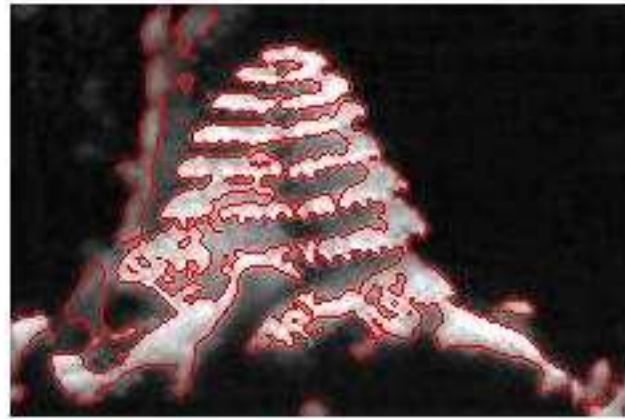
Other parameters remain unchanged, following images depicts the results of super resolution and low resolution segmentation images.

Segmentation of super resolution image with RSF method(2008)



Iterations=1000,time step=0.10,mu=1,epsilon=.9,sigma=2.00,lambda1=1,lambda2=1

Segmentation of low resolution image with RSF method(2008)



Iterations=200,time step=0.10,mu=1,epsilon=.9,sigma=2.00,lambda1=1,lambda2=1

Figure 5.4: Segmentation of high resolution image (Up) and low resolution image(Down)

5.3.5 Example 5

The super resolution and Low resolution Image size: 256×398

The motion parameters are considered as below:

Radiation:

All radiation parameters are set to zero.

Shift in x direction:

$t_{x1} = 0.0; t_{x2} = 0.82; t_{x3} = 0.11; t_{x4} = 0.70; t_{x5} = 0.55; t_{x6} = 0.097; t_{x7} = 0.26; t_{x8} = 0.50; t_{x9} = 0.74; t_{x10} = 0.86$

Shift in y direction:

$t_{y1} = 0.0; t_{y2} = 0.90; t_{y3} = 0.62; t_{y4} = 0.30; t_{y5} = 0.58; t_{y6} = 0.1; t_{y7} = 0.33; t_{y8} = 0.77; t_{y9} = 0.57; t_{y10} = 0.85$

Other parameters remain unchanged, following images depicts the results of super resolution and low resolution segmentation images.

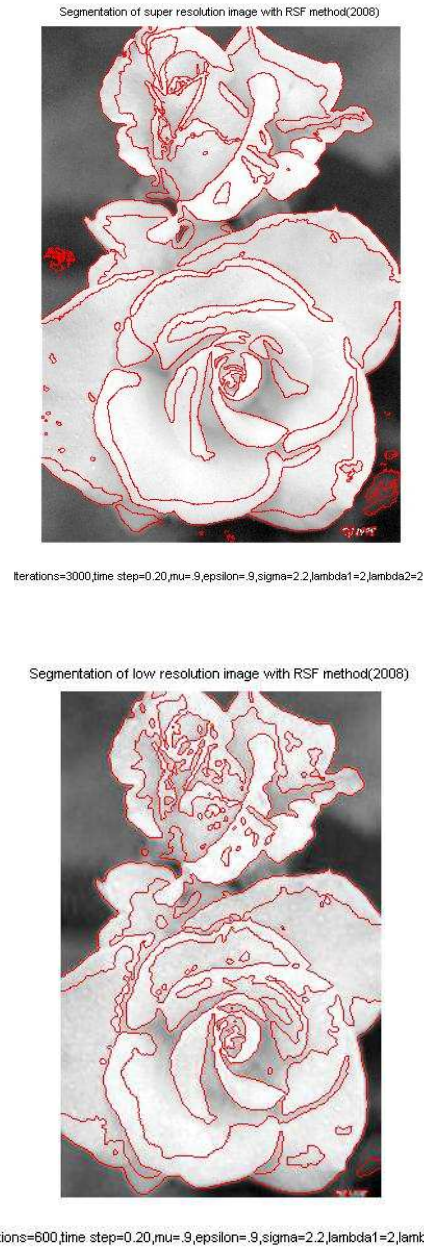


Figure 5.5: Segmentation of high resolution image (Up) and low resolution image(Down)

5.3.6 Example 6

The super resolution and Low resolution Image size: 290×215

The motion parameters are considered as below:

Radiation:

$R_1 = 0.0; R_2 = 0.0; R_3 = 0.0; R_4 = 0.0; R_5 = 0.0; R_6 = 0.0; R_7 = 0.8; R_8 = 0.0; R_9 = 0.0, R_{10} = 0.0$.

Shift in x direction:

$t_{x1} = 0.0; t_{x2} = 0.01; t_{x3} = 0.21; t_{x4} = 0.05; t_{x5} = 0.09; t_{x6} = 0.73; t_{x7} = 0.68; t_{x8} = 0.30; t_{x9} = 0.05; t_{x10} = 0.79$

Shift in y direction:

$t_{y1} = 0.0; t_{y2} = 0.32; t_{y3} = 0.69; t_{y4} = 0.80; t_{y5} = 0.17; t_{y6} = 0.41; t_{y7} = 0.45; t_{y8} = 0.63; t_{y9} = 0.60; t_{y10} = 0.75$

Other parameters remain unchanged, following images depicts the results of super resolution and low resolution segmentation images.

Segmentation of super resolution image with RSF method(2008)



Iterations=1000,time step=0.10,mu=1,epsilon=.9,sigma=2.0,lambda1=1,lambda2=1

Segmentation of low resolution image with RSF method(2008)



Iterations=500,time step=0.150,mu=1,epsilon=.9,sigma=2.2,lambda1=1,lambda2=1

Figure 5.6: Segmentation of high resolution image (Up) and low resolution image(Down)

5.3.7 Example 7

The super resolution and Low resolution Image size: 195×155

The motion parameters are considered as below:

Radiation:

$R_1 = 0.0; R_2 = 0.0; R_3 = 0.0; R_4 = -0.1; R_5 = 0.0; R_6 = 0.0; R_7 = 0.0; R_8 = 0.0; R_9 = -0.1; R_{10} = -0.1$.

Shift in x direction:

$t_{x1} = 0.0; t_{x2} = 0.055; t_{x3} = 0.18; t_{x4} = 0.013; t_{x5} = 0.07; t_{x6} = 0.75; t_{x7} = 0.50; t_{x8} = 0.24; t_{x9} = 0.79; t_{x10} = -0.1$

Shift in y direction:

$t_{y1} = 0.0; t_{y2} = 0.51; t_{y3} = 0.86; t_{y4} = 0.85; t_{y5} = 0.18; t_{y6} = 0.56; t_{y7} = 0.58; t_{y8} = 0.72; t_{y9} = 0.77; t_{y10} = 0.82$

Other parameters remain unchanged, following images depicts the results of super resolution and low resolution segmentation images.

Segmentation of super resolution image with RSF method(2008)



iterations=800,time step=0.10,mu=1,epsilon=.9,sigma=2.0,lambda1=1,lambda2=

Segmentation of low resolution image with RSF method(2008)



iterations=600,time step=0.15,mu=1,epsilon=.9,sigma=2.2,lambda1=1,lambda2=

Figure 5.7: Segmentation of high resolution image (Up) and low resolution image(Down)

5.3.8 Example 8

The super resolution and Low resolution Image size: 160×178

The motion parameters are considered as below:

Radiation:

$R_1 = 0.0; R_2 = 0.0; R_3 = 0.0; R_4 = 0.0; R_5 = 0.0; R_6 = 0.0; R_7 = -0.1; R_8 = 0.0; R_9 = 0.0, R_{10} = 0.0$.

Shift in x direction:

$t_{x1} = 0.0; t_{x2} = 0.2531; t_{x3} = 0.0361; t_{x4} = 0.6457; t_{x5} = 0.4233; t_{x6} = 0.1141; t_{x7} = 0.2049; t_{x8} = 0.3351; t_{x9} = 0.5310; t_{x10} = 0.2612$

Shift in y direction:

$t_{y1} = 0.0; t_{y2} = 0.3316; t_{y3} = 0.6701; t_{y4} = 0.253; t_{y5} = 0.5243; t_{y6} = 0.0687; t_{y7} = 0.2842; t_{y8} = 0.6764; t_{y9} = 0.3709; t_{y10} = 0.2766$

Other parameters remain unchanged, following images depicts the results of super resolution and low resolution segmentation images.

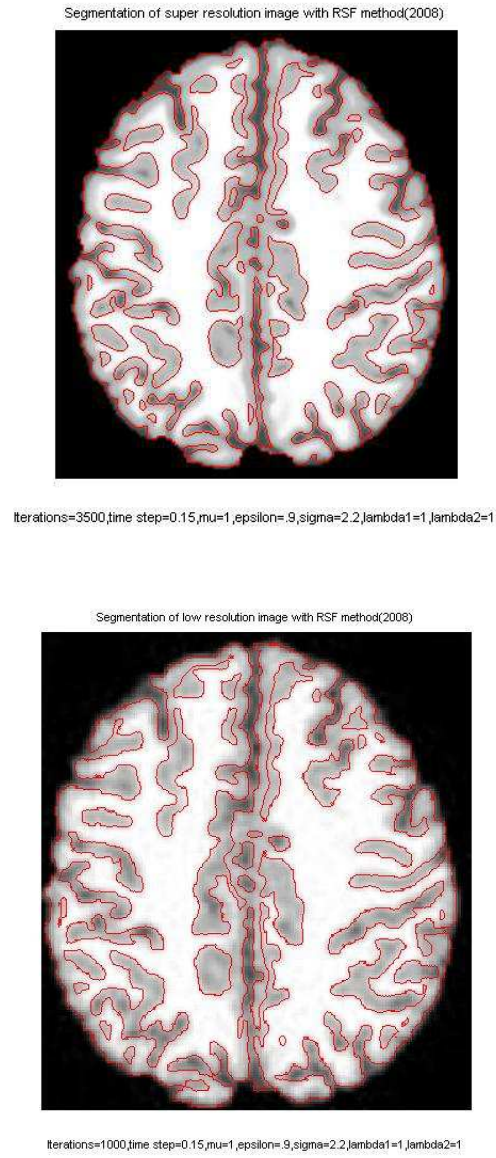


Figure 5.8: Segmentation of high resolution image (Up) and low resolution image(Down)

5.3.9 Example 9

The super resolution and Low resolution Image size: 178×217

The motion parameters are considered as below:

Radiation:

$R_1 = 0.0; R_2 = -0.1; R_3 = -0.1; R_4 = -0.1; R_5 = -0.1; R_6 = -0.1; R_7 = -0.1; R_8 = -0.1; R_9 = -0.10, R_{10} = -0.1$

Shift in x direction:

$t_{x1} = 0.0; t_{x2} = 0.4851; t_{x3} = 0.8031; t_{x4} = 0.1993; t_{x5} = 0.3908; t_{x6} = 0.8932; t_{x7} = 0.8874; t_{x8} = 0.9575; t_{x9} = 0.6335; t_{x10} = 0.0465$

Shift in y direction:

$t_{y1} = 0.0; t_{y2} = 0.9213; t_{y3} = 0.6554; t_{y4} = 0.5700; t_{y5} = 0.5986; t_{y6} = 0.3395; t_{y7} = 0.4611; t_{y8} = 0.1620; t_{y9} = 0.6343; t_{y10} = -0.0280$

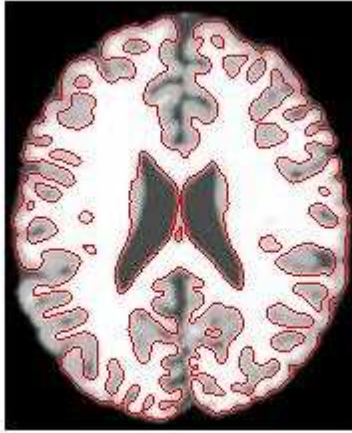
Other parameters remain unchanged, following images depicts the results of super resolution and low resolution segmentation images.

Segmentation of super resolution image with RSF method(2008)



ns=3000,time step=0.15,mu=1.0,epsilon=.9,sigma=2.2,lambda1=1,lambda2=1

Segmentation of low resolution image with RSF method(2008)



ns=3000,time step=0.15,mu=1.0,epsilon=.9,sigma=2.2,lambda1=1,lambda2=1

Figure 5.9: Segmentation of high resolution image (Up) and low resolution image(Down)

5.3.10 Example 10

The super resolution and Low resolution Image size: 174×208

The motion parameters are considered as below:

Radiation:

$R_1 = 0.0; R_2 = -0.1; R_3 = -0.1; R_4 = -0.1; R_5 = -0.1; R_6 = -0.1; R_7 = -0.1; R_8 = -0.1; R_9 = -0.10, R_{10} = -0.1$

Shift in x direction:

$t_{x1} = 0.0; t_{x2} = 0.4007; t_{x3} = 0.1514; t_{x4} = 0.2483; t_{x5} = 0.4856; t_{x6} = 0.5621; t_{x7} = 0.6646; t_{x8} = 0.6265; t_{x9} = 0.4269; t_{x10} = 0.0560$

Shift in y direction:

$t_{y1} = 0.0; t_{y2} = 0.7462; t_{y3} = 0.00698; t_{y4} = 0.6504; t_{y5} = 0.5463; t_{y6} = 0.9157; t_{y7} = 0.0767; t_{y8} = 0.3686; t_{y9} = 0.09103; t_{y10} = 0.7541$

Other parameters remain unchanged, following images depicts the results of super resolution and low resolution segmentation images.

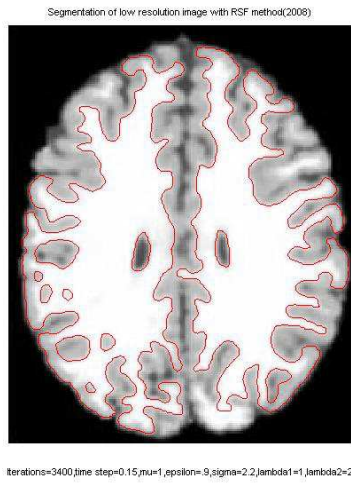


Figure 5.10: Segmentation of high resolution image (Up) and low resolution image(Down)

5.3.11 Example 11

The super resolution and Low resolution Image size: 178×216

The motion parameters are considered as below:

Radiation:

$R_1 = 0.0; R_2 = 0.0; R_3 = 0.0; R_4 = 0.0; R_5 = 0.0; R_6 = 0.0; R_7 = 0.0; R_8 = -0.1; R_9 = 0.0, R_{10} = 0.0$

Shift in x direction:

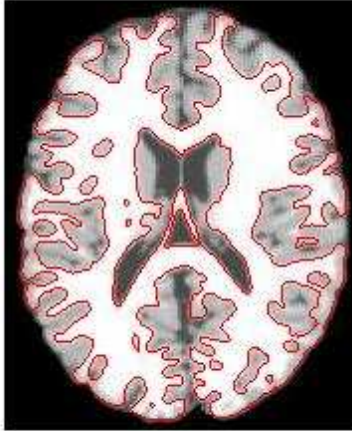
$t_{x1} = 0.0; t_{x2} = 0.9056; t_{x3} = 0.0948; t_{x4} = 0.8182; t_{x5} = 0.5997; t_{x6} = 0.1076; t_{x7} = 0.2689; t_{x8} = 0.5300; t_{x9} = 0.8897; t_{x10} = 0.9689$

Shift in y direction:

$t_{y1} = 0.0; t_{y2} = 0.9690; t_{y3} = 0.8424; t_{y4} = 0.3343; t_{y5} = 0.7123; t_{y6} = 0.0926; t_{y7} = 0.3537; t_{y8} = 0.8464; t_{y9} = 0.6793; t_{y10} = 0.9532$

Other parameters remain unchanged, following images depicts the results of super resolution and low resolution segmentation images.

Segmentation of super resolution image with RSF method(2008)



ns=1500,time step=0.15,mu=1.0,epsilon=.9,sigma=2.2,lambda1=1,lambda2=1

Segmentation of low resolution image with RSF method(2008)



ns=1500,time step=0.15,mu=1.0,epsilon=.9,sigma=2.2,lambda1=1,lambda2=1

Figure 5.11: Segmentation of high resolution image (Up) and low resolution image(Down)

5.3.12 Example 12

The super resolution and Low resolution Image size: 178×216

The motion parameters are considered as below:

Radiation:

All radiation parameters are set to zero.

Shift in x direction:

$t_{x1} = 0.0; t_{x2} = 0.3047; t_{x3} = 0.1371; t_{x4} = 0.7770; t_{x5} = 0.5779; t_{x6} = 0.1094; t_{x7} = 0.2707; t_{x8} = 0.5325; t_{x9} = 0.8601; t_{x10} = 0.9575$

Shift in y direction:

$t_{y1} = 0.0; t_{y2} = 0.9718; t_{y3} = 0.8522; t_{y4} = 0.2042; t_{y5} = 0.4480; t_{y6} = 0.2055; t_{y7} = 0.3785; t_{y8} = 0.9041; t_{y9} = 0.7227; t_{y10} = 0.9572$

Other parameters remain unchanged, following images depicts the results of super resolution and low resolution segmentation images.

Segmentation of super resolution image with RSF method(2008)



ns=5000,time step=0.15,mu=1.0,epsilon=.9,sigma=2.2,lambda1=1,lamb

Segmentation of low resolution image with RSF method(2008)



ns=5000,time step=0.15,mu=1.0,epsilon=.9,sigma=2.2,lambda1=1,lamb

Figure 5.12: Segmentation of high resolution image (Up) and low resolution image(Down)

By comparing segmentation results of low resolution and super resolution images it can be concluded that super resolution images has far so better results in facing to segmentation.

As it is mentioned earlier, segmentation is a process of partitioning a digital image into homogeneous and meaningful regions that play a pivotal role in the field of image analysis in application such as automatic target recognition. But, if the the image detector array is not dense enough, the resulting images are degraded. Also, discretizing process and blurring factors limit reliable segmentation.

However, when segmentation is applied in super resolution images, it improves the quality of the images and reduce or completely eliminate the aliasing.

Actually, in segmentation process edge detection is highly demanded to establish precise border.

6

Conclusion

Super resolution is a process of producing high resolution images through several low resolution images that are noisy, blurred and down sampled.

Moreover, image segmentation is to cluster pixels into salient image regions.

Actually, image segmentation is partitioning a specific image into several meaningful regions corresponding to natural parts of objects and individual surfaces.

The concept of image segmentation started around 1970. But, there is still no robust solution toward it, because of contrast variety of images is too large. Furthermore, there is the lack of standard benchmark to judge the segmented images.

Segmentation accuracy is inherently limited by the resolution of the acquired images. Because of some reasons such as limitations of the used hardware, an image does not have acceptable resolution.

The objective of this thesis was to find an appropriate approach to improve segmentation. In this way, images first processed by super resolution software, and then send to segmentation part.

The images used in this thesis, are two different types of images one is normal image and another is magnetic resonance (MR) images. Due to different properties and characteristics in these two types of images two different types of parameters are applied to them.

According to chapter 5, by comparison of the performance of segmentation of super resolution images with low resolution images we get to the conclusion that super resolution images, segmented slightly better than low resolution images.

Bibliography

- [1] S. Park, M. Park, M. Kang, Super resolution image reconstruction, IEEE Signal Processing Magazine 20 (3) (2003) 21–36.
- [2] C. Hendricks, L. Vliet, Improvement resolution to reduce aliasing in an under sampled image sequence, In Proc. SPIE , Electronic Imaging 2000 Conference, San Jose 3965A (2000) 214–222.
- [3] X. Gao, D. Tao, B. Ning, X. Li, A multiframe image super resolution method, Signal Processing,Elsevier 90 (2) (2009) 405–414.
- [4] R. Tsai, T. Huang, Multi-frame image restoration and registration, Advances in computer vision and image processing,volume 1,Chapter 7, 317-339.
- [5] B. Tom, A. Akatsaggelos, N. Galatsanos, Reconstruction of a high resolution image from multiple degraded low resolution images, In Proc. IEEE Int. Conf. in Image processing,IEEE 3 (1994) 553–557.
- [6] P. Vandewalle, S. Susstrunk, M. Vetterli, Frequency domain approach to registration of aliased images with application to super resolution, EURASIP Journal on applied signal processing 2006 (2006) Article ID 71459.
- [7] P. Vandewalle, M. Rumo, Super resolution in image using optical flow and irregular sampling.
- [8] R. Schultz, R. Stevansson, Extraction of high resolution frames from video sequences, IEEE Transaction on image processing 5 (6) (1996) 996–1011.
- [9] H. Stark, P. Askoui, High resolution image recovery from image plane arrays, using convex projection, JOSA A (1989), 11, 1715-1726.
- [10] A. Tekalp, M. Zkan, M. Sezan, High resolution image reconstruction from lower resolution image sequences and space varying image registration, IEEE Int. Conf. acoustics, speech and signal processing, ICASSP, San Francisco, CA 3 (1992) 169–172.

- [11] P. Miklos, Image interpolation techniques, 2nd Serbian-Hungarian Joint Symposium on intelligent systems, Sabotica, Serbia and Montenegro, October, 2004.
- [12] M. Protter, M. Elad, H. Takeda, P. Milanfar, Generalizing the nonlocal-means to super resolution construction, *IEEE Trans. on image processing Image Processing* 18 (1) (2009) 36–51.
- [13] N. Joshi, C. Zitnick, R. Szelisk, D. Kriegman, Image deblurring and denoising using color priors, *Computer vision and pattern recognition ,CVPR 2009.IEEE* (1) (2009) 1550–1557.
- [14] J. Lie, M. Lyskar, X. Tai, A binary model and and some applications to mumford shah image segmentation, *IEEE Transaction on image processing* 15 (5) (2004) 1171–1181.
- [15] H. Demirel, S. Izadpanahi, M. Anbarjafari, Improved motion based localized super resolution technique using discrete wavelet transform for low resolution video enhancement, 17th. European signal processing conference, EUSIPCO 2009, Glasgow, Scotland 1097–1101.
- [16] P. Chatterjeel, S. Mukherjeel, S. Chaudurri, G. Seetharman, Application of papoulis-grechberg method in image super-resolution inpainting, *The computer journal* 52 (1) (2009) 80–89.
- [17] M. Irani, S. Peleg, Motion analysis for image enhancement: Resolution, occlusion and transparency, *Journal of visual communications* 4 (1993) 324–355.
- [18] S. Farsiu, M. Robinson, M. Elad, P. Milanfar, Fast and robust multiframe super resolution, *IEEE Trans. Image process.* 13 (10) (2004) 1327–1344.
- [19] A. Zomet, A. Rav-Acha, S. Pelag, Robust super resolution, *Proc. Int. Conf. Computer vision and pattern recognition* 1 (2001) 645–650.
- [20] A. Patti, M. Sezan, A. Tekalp, High resolution image reconstruction from a low resolution image sequence of time varying motion blur, In *Proc. of the Int. Conf. on accoustic speech and signal proc.*, San Francisco, CA., IEEE 1 (1992) 23–26.
- [21] T. Pham, L. Vliet, K. Schutte, Robust fusion of irregularity sampled data using adaptive normalized convolution, *EURASIP Journal on applied signal processing*, May 2005 1-12.
- [22] C. Li, C. Kao, J. Gore, Z. Ding, Minimization of region scalable fitting energy for image segmentation, *IEEE Transactions on image processing* 17 (10) (2008) 1940–1949.
- [23] M. L. A. Nazif, An experimental rule based system for testing low level segmentation techniques, Academic. Press, Cambridge, U.K., 1982.

- [24] M. Sharma, Performance evolution of image segmentation and texture extraction, Ph.D. thesis, Doctoral dissertation (U.K), Exter University (2001).